Method for the modulation of cancer treatment based on analyzing the gut microbiome

Panagiotou, Gianni; Heshiki, Yoshitaro; Vazquez-Uribe, Ruben; Quainoo, Scott; Sommer, Morten; Weiss, Glen

Publication date:
2021

Document Version
Publisher's PDF, also known as Version of record

(12) INTERNATIONAL APPLICATION PUBLISHED UNDER THE PATENT COOPERATION TREATY (PCT)

(19) World Intellectual Property Organization
International Bureau

(43) International Publication Date
10 September 2021 (10.09.2021)

WIPO | PCT

(10) International Publication Number
WO 2021/176036 A1

(51) International Patent Classification:
C12Q 1/6886 (2018.01) *C12Q 1/689* (2018.01)

(21) International Application Number:
PCT/EP2021/055556

(22) International Filing Date:
05 March 2021 (05.03.2021)

(25) Filing Language: English

(26) Publication Language: English

(30) Priority Data:
62/986,063 06 March 2020 (06.03.2020) US

(71) Applicants: **LEIBNIZ-INSTITUT FÜR NATURSTOFF-FORSCHUNG UND INFEKTIONSBIOLOGIE E. V. HANS-KNÖLL-INSTITUT (HKI)** [DE/DE]; Beutenbergstraße 11a, 07745 Jena (DE). **DANMARKS TEKNISKE UNIVERSITET** [DK/DK]; Anker Engelunds Vej 1 Bygning 101A, 2800 Kgs. Lyngby (DK).

(72) Inventors: **PANAGIOTOU, Gianni**; Knaackstrasse 35, 10405 Berlin (DE). **HESHIKI, Yoshitaro**; #905, 2-17-18 Daita, Setagaya-ku, Tokyo, 155-0033 (JP). **VAZQUEZ-URIBE, Ruben**; Hollændervej 23a, 1855 Frederiksberg (DK). **QUAINOO, Scott**; H. P. Ørums Gade 20, 2100 København (DK). **SOMMER, Morten, Otto, Alexander**; Duntzfelts Alle 22, 2900 Hellerup (DK). **WEISS, Glen**; 665 Washington St. #1015, Boston, Massachusetts 02111 (US).

(74) Agent: **KRAUSS, Jan, B.,**; Boehmert & Boehmert Anwaltspartnerschaft mbB, Pettenkoferstrasse 22, 80336 Munich (DE).

(81) Designated States *(unless otherwise indicated, for every kind of national protection available)*: AE, AG, AL, AM, AO, AT, AU, AZ, BA, BB, BG, BH, BN, BR, BW, BY, BZ, CA, CH, CL, CN, CO, CR, CU, CZ, DE, DJ, DK, DM, DO, DZ, EC, EE, EG, ES, FI, GB, GD, GE, GH, GM, GT, HN, HR, HU, ID, IL, IN, IR, IS, IT, JO, JP, KE, KG, KH, KN, KP, KR, KW, KZ, LA, LC, LK, LR, LS, LU, LY, MA, MD, ME, MG, MK, MN, MW, MX, MY, MZ, NA, NG, NI, NO, NZ, OM, PA, PE, PG, PH, PL, PT, QA, RO, RS, RU, RW,

(54) Title: METHOD FOR THE MODULATION OF CANCER TREATMENT BASED ON ANALYZING THE GUT MICROBIOME

Figure 1

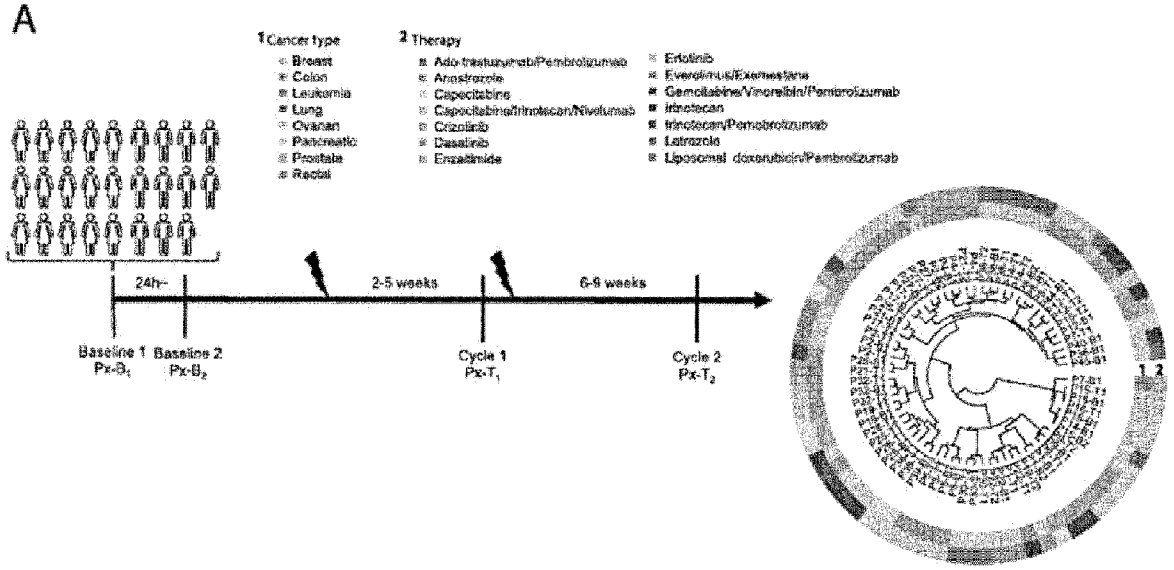

(57) Abstract: The present invention relates to a method for prognosing a response to a cancer therapy in a human patient, comprising the steps of a) detecting the alpha diversity of the gut microbiome in a sample obtained from said human patient, and b) prognosing the response to cancer therapy in said human patient, wherein a higher alpha diversity of the gut microbiome of said patient is indicative for a response to said cancer therapy, when compared to a non-responsive patient. The present invention further relates to improved treatment strategies for cancer based on the alpha diversity of the gut microbiome.

WO 2021/176036 A1

[Continued on next page]

SA, SC, SD, SE, SG, SK, SL, ST, SV, SY, TH, TJ, TM, TN, TR, TT, TZ, UA, UG, US, UZ, VC, VN, WS, ZA, ZM, ZW.

(84) **Designated States** *(unless otherwise indicated, for every kind of regional protection available)*: ARIPO (BW, GH, GM, KE, LR, LS, MW, MZ, NA, RW, SD, SL, ST, SZ, TZ, UG, ZM, ZW), Eurasian (AM, AZ, BY, KG, KZ, RU, TJ, TM), European (AL, AT, BE, BG, CH, CY, CZ, DE, DK, EE, ES, FI, FR, GB, GR, HR, HU, IE, IS, IT, LT, LU, LV, MC, MK, MT, NL, NO, PL, PT, RO, RS, SE, SI, SK, SM, TR), OAPI (BF, BJ, CF, CG, CI, CM, GA, GN, GQ, GW, KM, ML, MR, NE, SN, TD, TG).

Published:

— *with international search report (Art. 21(3))*

— *with sequence listing part of description (Rule 5.2(a))*

Method for the modulation of cancer treatment based on analyzing the gut microbiome

The present invention relates to a method for prognosing a response to a cancer therapy in a human patient, comprising the steps of a) detecting the alpha diversity of the gut microbiome in a sample obtained from said human patient, and b) prognosing the response to cancer therapy in said human patient, wherein a higher alpha diversity of the gut microbiome of said patient is indicative for a response to said cancer therapy, when compared to a non-responsive patient. The present invention further relates to improved treatment strategies for cancer based on the alpha diversity of the gut microbiome.

Background of the invention

Cancer is one of the leading causes of mortality worldwide, with nearly one in six deaths globally attributed to cancer [1]. Among several treatment options, chemotherapy and immunotherapy are applied to treat cancer by preventing cancer cell division or boosting the immune system to eliminate cancerous cells [2]. In spite of recent progress, treatment outcomes are still unsatisfactory for most cancer types.

The gut microbiota is increasingly considered an important factor associated with both tumor development and the efficacy of anti-cancer therapies [3]. Specific gut bacteria have been shown to affect cancer treatments through direct drug metabolism and modulation of the host immune response [4]. Bacterial beta-glucuronidase can convert irinotecan, an anti-cancer chemotherapy drug, to a toxic metabolite [5], and intratumor bacterial cytidine deaminase can degrade gemcitabine with a direct impact on treatment outcomes [6]. The gut microbiota or defined synthetic communities can also impact treatment outcomes through immune modulation mechanisms such as regulating T cell differentiation [7–9]. Indeed, the gut microbiota can substantially affect immune checkpoint inhibitor therapy [10–13] and antibiotic use is associated with poor treatment outcomes with checkpoint inhibitors [14].

Obtaining a comprehensive view of the microbial ecosystem in the patient's gut – the microbiome – has become possible with high-throughput environmental shotgun sequencing techniques (Human Microbiome Project Consortium, 2012; Qin et al., 2010), and first associations of microbiota with disease have been reported, such as obesity, type II diabetes, and atherosclerosis (e.g. Karlsson et al., 2013; Le Chatelier et al., 2013; Qin et al., 2012; Turnbaugh et al., 2009).

It is therefore an object of the present invention to provide improved means and methods for the diagnosis and prognosis as well as for the treatment of cancer, based on the gut microbiome. Other objects of the present invention will become apparent to the person of skill when studying the specification of the present invention.

In a first aspect thereof, the object of the present invention is solved by providing a method for prognosing a response to a cancer therapy in a human patient, comprising the steps of a) detecting the alpha diversity of the gut microbiome in a sample obtained from said human patient, and b) prognosing the response to cancer therapy in said human patient, wherein a higher alpha diversity of the gut microbiome of said patient is indicative for a response to said cancer therapy, when compared to a non-responsive patient.

In the context of the method according to the present invention, said prognosing a response shall refer to a situation where a sample is taken from a patient before a cancer treatment (i.e. an initial sample) as well as a sample is taken during or after the course of said treatment. It was found that the present method can be prognostic both for a likelihood of an overall therapy response, as well as for a response of the course of a treatment as applied.

The inventors used the relative abundances at the baseline of 31 differentially abundant species between R and NR (Fig. 1g) and the baseline RPKM of the differentially abundant KEGG pathways (Fig. 3b). Therefore, in one embodiment of the present method according to the present invention, therefore, KEGG pathways are included in the analysis, and a statistical analysis of the KEGG pathways as identified in said sample(s) combined with the above method is preferably performed. The model

performance was evaluated with an area under the curve (AUC) of receiver operating characteristic (ROC). The model incorporating data on both species and pathways showed the best performance (AUC = 0.895), indicating the power of shotgun metagenomics for predicting host phenotypes. To further test the general applicability of the model, the inventors recruited additional cancer patients and performed metagenomics sequencing in seven more patients (baseline samples from R = 5, NR = 2) to serve as an independent validation dataset. Using the initial relative abundance of differentially abundant species and the RPKM of differentially abundant KEGG pathways, the inventors could achieve an AUC = 0.75. Therefore, preferred is a method with a performance of AUC < 0.75.

Preferred is also a method according to the present invention, further comprising monitoring the progress of said cancer therapy based on said response as detected

Previous studies have focused on elucidating the role of individual microbes or communities in a specific cancer type and therapeutic intervention. In the present invention, the inventors investigated the role of gut microbiota in a cancer patient cohort that included eight different cancer types treated with either cytotoxic or targeted chemotherapy, immunotherapy, or a combination. The inventor's objective here was to demonstrate a more global finding of a microbiota signature that is independent of cancer type and heterogeneity. Using a combination of human feces shotgun metagenomic sequencing, in vitro and in vivo mouse models, the inventors found that cancer treatment outcomes in this diverse cohort can be substantially modulated by the abundances of specific gut bacteria, supporting a recent study in healthy individuals to identify general activators of the immune system [15].

The gut microbiota has the potential to influence the efficacy of cancer therapy. In the present invention, the inventors investigated the contribution of the intestinal microbiome on treatment outcomes in a heterogeneous cohort that included multiple cancer types to identify microbes with a global impact on immune response. Human gut metagenomic analysis revealed that responder patients had significantly higher microbial diversity and different microbiota compositions compared to non-responders. A machine-learning model was developed and validated in an independent cohort to

predict treatment outcomes based on gut microbiota composition and functional repertoires of responders and non-responders. Specific species, Bacteroides ovatus and Bacteroides xylanisolvens, were positively correlated with treatment outcomes. Oral gavage of these responder bacteria significantly increased the efficacy of erlotinib and induced the expression of CXCL9 and IFN-γ in a murine lung cancer model. These data suggest a predictable impact of specific constituents of the microbiota on tumor growth and cancer treatment outcomes with implications for both prognosis and therapy.

The inventive methods can also be performed on samples derived from the fecal sample, as long as the composition of the gut microbiome can be reliably determined. Thus, optimally, the samples should be obtained and maintained using procedures that avoid harsh treatments of the samples, in order to maintain the composition of the strains as analyzed to as much as possible. Factors that should be monitored are, amongst others, temperature, humidity, and contact with air (oxygen). Suitable sampling methods are known to the person of skill (e.g. as described herein), and can be identified by the person of skill without any undue burden. The inventive methods can also be performed on a sample as obtained from said patient, e.g. on a sample as taken and suitably stored for later analysis.

Preferred is the method according to the present invention, wherein said sample is taken before said treatment as initial sample, or during said treatment.

Preferred is the method according to the present invention, further comprising detecting an increase of the abundance of at least one of the species of at least one of Bacteroides xylanisolves, Bacteroides ovatus, Prevotella copri, Alistipes finegoldii, Bacteroides faecis, Bacteroides intestinalis, Biophila wadsworthia, Alistipes indistinctus, Colinsella aerofaciens, Alistipes shahii, Odoribacter splanchnicus, Alistipes putredinis, Bacteriodales bacterium ph8, Eubacterium rectale, Alistipes sp AP11, Parasutterella excrementihominis, Alistipes onderdonkii, Desulfovibrio desulfuricans, Eubacterium ventriosum, Bacteroides fragilis, and Coprococcus cornes in said sample, in particular Bacteroides xylanisolves, and Bacteroides ovatus; and Lachnospiraceae bacterium 5 1 57FAA, Lachnospiraceae bacterium 3 1 57FAA CT1, Clostridium spiroforme, Clostridium symbiosum, Anaerotruncuis colihominis, Ruminococcus gnavus,

Clostridium hathewayi, Clostridales bacterium 1 7 47FAA, and Erysipelotrichaceae bacterium 21 3 in said sample, in particular Clostridium symbiosum, and Ruminococcus gnavus. These species can add even further significance to the methods of the invention. Most preferred is the detection of all species as listed.

Preferred is the method according to the present invention, wherein said cancer is selected from breast, colon, lung, ovarian, pancreatic, prostate, and rectal cancer and leukemia.

Yet another aspect of the present invention then relates to a method according to the present invention, further comprising combining said test with a method selected from detecting the level of expression of KEGG (Kyoto Encyclopedia of Genes and Genomes) module markers, amount (abundance) or expression of CAZy (Carbohydrate-Active enZYmes database) family markers. Preferred KEGG module markers and CAZy markers are selected from markers (e.g. genes) involved in the LPS metabolism, such as, for example, listed in Figure 3.

For measuring and/or detecting of the alpha diversity of the gut microbiome as described herein as well as the species as described, standard methods can be used, such as, for example, a method selected from the group of detecting the alpha diversity of the gut microbiome comprises at least one of microbiome antigenic profiling, shotgun metagenomic sequencing, PCR, rtPCR, qPCR, multiplex PCR, high-throughput sequencing, metatranscriptomic sequencing, identification of strain-specific markers, such as genes and/or proteins, and 16S rDNA analysis. These methods also include enzymatic tests in order to identify functional changes as long as these changes for allow a species-specific analysis. The test may also be quantitative.

Preferred is the method according to the present invention, wherein said patient is undergoing treatment for cancer, such as breast, colon, lung, ovarian, pancreatic, prostate, and/or rectal cancer and/or leukemia. Said treatment can preferably be performed as described below, and can be selected from at least one of a cytotoxic, targeted, and immunotherapy of said patient.

Preferred is the method according to the present invention, wherein said higher alpha diversity in the responding patient is significantly higher, as indicated by a $p < 0.01$, preferably $p < 0.005$ in a Wilcoxon-rank-sum test.

Preferred is the method according to the present invention, wherein the responding patient exhibits a significantly lower ratio of the phylii Firmicutes/Bacteroidetes (F/B) in said sample.

Further preferred is the method according to the present invention, wherein the responding patient exhibits a significant enrichment of at least one of Bacteroides xylanisolves, Bacteroides ovatus, Prevotella copri, Alistipes finegoldii, Bacteroides faecis, Bacteroides intestinalis, Biophila wadsworthia, Alistipes indistinctus, Colinsella aerofaciens, Alistipes shahii, Odoribacter splanchnicus, Alistipes putredinis, Bacteriodales bacterium ph8, Eubacterium rectale, Alistipes sp AP11, Parasutterella excrementihominis, Alistipes onderdonkii, Desulfovibrio desulfuricans, Eubacterium ventriosum, Bacteroides fragilis, and Coprococcus cornes in said sample, in particular Bacteroides xylanisolves, and Bacteroides ovatus; and wherein the non-responding patient exhibits a significant enrichment of at least one of Lachnospiraceae bacterium 5 1 57FAA, Lachnospiraceae bacterium 3 1 57FAA CT1, Clostridium spiroforme, Clostridium symbiosum, Anaerotruncuis colihominis, Ruminococcus gnavus, Clostridium hathewayi, Clostridales bacterium 1 7 47FAA, and Erysipelotrichaceae bacterium 21 3 in said sample, in particular Clostridium symbiosum, and Ruminococcus gnavus.

As mentioned above, said sample can be taken before said treatment as initial sample, or during said treatment.

Yet another aspect of the present invention then relates to a method for monitoring the progress of said cancer therapy based on said response as detected using a method as described above. After detecting the alpha diversity of the gut microbiome in a sample obtained from said human patient undergoing therapy, the attending physician can prognose or identify the response to said cancer therapy in said human patient based on whether a higher alpha diversity of the gut microbiome of said patient is found

compared to an earlier or control sample, which is indicative for a response to said cancer therapy. The therapy can then be adjusted accordingly, e.g. switched to a new drug or treatment schedule, and/or increasing the diversity of the gut microbiome as disclosed herein.

Preferred is the method according to the present invention, further comprising combining said test with a method selected from detecting the abundance or expression of KEGG module markers, amount, abundance or expression of CAZy family markers.

In addition to the above approaches, new targets for a better cancer therapy are desired. Thus, according to another aspect thereof, the present invention provides a method for detecting and/or identifying a compound suitable for the treatment of cancer, comprising the steps of
a) administering a candidate compound to a mammalian cancer patient, and
b) detecting the alpha diversity of the gut microbiome in a sample obtained from said mammalian cancer patient, and c) identifying a compound as suitable for the treatment of cancer if a higher alpha diversity of the gut microbiome of said patient is detected in the presence of said compound when compared to the absence of said compound. Preferably steps a) to c) can be repeated, and, optionally, said compound can be chemically modified (where possible) before said repeating.

The mammal and/or patient can be a rat, mouse, goat, rabbit, sheep, horse, monkey or human, preferred is a mouse, rat or human. Most preferred is a mouse.

More preferred is a method for detecting and/or identifying according to the present invention, wherein said compound is selected from the group consisting of a peptide library, a combinatory library, a cell extract, in particular a plant cell extract, a “small molecular drug”, an antisense oligonucleotide, an siRNA, an mRNA and an antibody or fragment thereof (such as Fab or scFv, and the like), a cytotoxic, targeted, immunotherapeutic compound, and a composition comprising at least one bacterial species Bacteroides xylanisolves, Bacteroides ovatus, Prevotella copri, Alistipes finegoldii, Bacteroides faecis, Bacteroides intestinalis, Biophila wadsworthia, Alistipes indistinctus, Colinsella aerofaciens, Alistipes shahii, Odoribacter splanchnicus, Alistipes

putredinis, Bacteriodales bacterium ph8, Eubacterium rectale, Alistipes sp AP11, Parasutterella excrementihominis, Alistipes onderdonkii, Desulfovibrio desulfuricans, Eubacterium ventriosum, Bacteroides fragilis, and Coprococcus cornes, in particular Bacteroides xylanisolves, and Bacteroides ovatus.

Preferred is a method for detecting and/or identifying according to the present invention, further comprising testing said compound(s) as detected/identified for its cancer. Respective assays are known to the person of skill, and can be taken from the respective literature.

Preferred is a method for detecting and/or identifying according to the present invention, wherein steps a) to d) are repeated, and, optionally, chemically modifying said compound before said repeating. The thus identified candidate compound can then, in a preferred embodiment, modified in a further step. Modification can be effected by a variety of methods known in the art, which include, without limitation, the introduction of novel side chains or the exchange of functional groups like, for example, introduction of halogens, in particular F, Cl or Br, the introduction of lower alkyl groups, preferably having one to five carbon atoms like, for example, methyl, ethyl, n-propyl, isopropyl, n-butyl, isobutyl, tert-butyl, n-pentyl or iso-pentyl groups, lower alkenyl groups, preferably having two to five carbon atoms, lower alkynyl groups, preferably having two to five carbon atoms or through the introduction of, for example, a group selected from the group consisting of NH_2, NO_2, OH, SH, NH, CN, aryl, heteroaryl, COH or COOH group. The thus modified binding substances are than individually tested with a method of the present invention. If needed, the steps of selecting the candidate compound, modifying the compound, and testing compound can be repeated a third or any given number of times as required. The above described method is also termed ”directed evolution” since it involves a multitude of steps including modification and selection, whereby binding compounds are selected in an ”evolutionary” process optimizing its capabilities with respect to a particular property, e.g. its ability to act on cancer and/or its progression.

Preferred is a method for detecting and/or identifying according to the present invention, wherein said patient is undergoing treatment for cancer. Said treatment can preferably be performed as described below.

Another aspect of the present invention relates to a method for manufacturing a pharmaceutical composition for cancer, comprising the steps of: performing a method for detecting and/or identifying according to the present invention, and formulating said compound as detected and identified into a pharmaceutical composition.

In a further embodiment of the method of the present invention, the compound identified as outlined above, which may or may not have gone through additional rounds of modification and selection, is admixed with suitable auxiliary substances and/or additives. Such substances comprise pharmacological acceptable substances, which increase the stability, solubility, biocompatibility, or biological half-life of the interacting compound or comprise substances or materials, which have to be included for certain routes of application like, for example, intravenous solution, sprays, band-aids or pills.

Carriers, excipients and strategies to formulate a pharmaceutical composition, for example to be administered systemically or topically, by any conventional route, in particular enterally, e.g. orally, e.g. in the form of tablets or capsules, parenterally, e.g. in the form of injectable solutions or suspensions, topically, e.g. in the form of lotions, gels, ointments or creams, or in nasal or a suppository form are well known to the person of skill and described in the respective literature.

Administration of an agent, e.g., a compound can be accomplished by any method which allows the agent to reach the target cells. These methods include, e.g., injection, deposition, implantation, suppositories, oral ingestion, inhalation, topical administration, or any other method of administration where access to the target cells by the agent is obtained. Injections can be, e.g., intravenous, intradermal, subcutaneous, intramuscular or intraperitoneal. Implantation includes inserting implantable drug delivery systems, e.g., microspheres, hydrogels, polymeric reservoirs, cholesterol matrices, polymeric systems, e.g., matrix erosion and/or diffusion systems and non-

polymeric systems, e.g., compressed, fused or partially fused pellets. Suppositories include glycerin suppositories. Oral ingestion doses can be enterically coated. Inhalation includes administering the agent with an aerosol in an inhalator, either alone or attached to a carrier that can be absorbed. The agent can be suspended in liquid, e.g., in dissolved or colloidal form. The liquid can be a solvent, partial solvent or non-solvent. In many cases, water or an organic liquid can be used.

Yet another aspect of the present invention is directed at a pharmaceutical composition for treating or preventing cancer, obtainable by a method according to the method as herein. Another aspect of the present invention relates to a pharmaceutical composition as described herein, wherein the pharmaceutical composition further comprises additional pharmaceutically active ingredients for treating cancer, such as, for example, cytotoxic active ingredients, targeted active ingredients, and/or immunotherapy, in particular kinase inhibitors, such as erlotinib.

Another aspect of the invention relates to a pharmaceutical composition comprising Bacteroides xylanisolves and/or Bacteroides ovatus for use in the treatment of cancer in a mammalian patient. Said treatment may comprise a combination treatment with a cytotoxic, targeted, and/or immunotherapy in said patient, in particular kinase inhibitors, such as erlotinib.

Another aspect of the present invention then relates to a method for treating or preventing cancer in a human patient in need thereof, comprising a method according to the present invention as described herein, wherein said treatment is – at least in part – adjusted to and/or based on a method as above and/or comprises administering a pharmaceutical composition comprising Bacteroides xylanisolves and/or Bacteroides ovatus to said patient, preferably as a combination treatment with a cytotoxic, targeted, and/or immunotherapy, in particular kinase inhibitors, such as erlotinib.

Preferred is a therapeutic method according to the present invention, comprising administering to said patient an effective amount of a compound as identified according to the present invention as described herein. In general, the attending physician will base a treatment on the compound as identified, and optionally also on other individual

patient data (clinical data, family history, DNA, etc.), and a treatment can also be performed based on the combination of these factors. Significant information about drug effectiveness, drug interactions, and other patient status conditions can be used, too.

Treatment is meant to include, e.g., preventing, treating, reducing the symptoms of, or curing the disease or condition, i.e. cancer. An "effective amount" is an amount of the compound(s) or the pharmaceutical composition as described herein that alleviates symptoms as found for cancer, such as, for example, frequency and/or size. Alleviating is meant to include, e.g., preventing, treating, reducing the symptoms of, or curing the disease (CRC and/or advanced adenomas) or condition. The invention also includes a method for treating a subject at risk for a development and/or progression of cancers, wherein a therapeutically effective amount of a compound as above is provided. Being at risk for the disease can result from, e.g., a family history of the disease, a genotype which predisposes to the disease, or phenotypic symptoms which predispose to the disease.

The inventors evaluated here for the first time the role of the gut microbiota in a heterogeneous patient cohort with various types of cancer and anticancer treatments to identify microbes with an impact on immune response. The inventors identified significant differences in the gut microbiota composition and functional repertoire between R and NR, which were highly associated with treatment efficacy. Based on shotgun metagenomic data, the inventors constructed and validated a statistical model that could predict cancer treatment outcomes with high accuracy in an independent validation cohort.

Despite the successful validation of the role of R-enriched bacteria in an animal model, the inventor's study comes also with limitations. First, while the response criteria were uniformly applied across treatment and cancer type as is typically performed in clinical trials, the likelihood of responsiveness may vary by line of therapy and clinical context. The inventors focused on the microbiota signature that differentiated based on clinical outcome, not the cancer type or therapy. Second, due to a relatively small number of patients, the inventors have also included a relatively small independent clinical cohort

of patients for validation of the microbiota signature. A larger cohort will definitely provide the chance to overcome the issues with potential confounding factors and facilitate the detailed investigations into the effects of cancer types and treatments on gut microbiota. However, even with a small cohort, a solid conclusion and/or a highly accurate predictive model could be made from the comparison between groups in recent gut microbiome studies [36–38]. The inventors also believe that mechanistic and biologic support for the inventor's findings from the clinical cohort was validated in the preclinical studies. Furthermore, future studies may investigate whether the NR-associated species can promote tumor growth and cancer progression in the absence of drug treatment, given the larger tumor size of NR + erlotinib group than the PBS + erlotinib group observed at day 10 (Fig. 4c). In addition, even though the functional analyses based solely on metagenomic data have shed lights on the potential mechanisms of gut microbiota affecting treatment outcomes, the use of metatranscriptomics and metabolomics to measure the actively expressed gut microbial functions and functional end-products, respectively, can lead to more robust and solid findings. Lastly, the murine experiment used erlotinib, an EGFR tyrosine kinase inhibitor, and not a cytotoxic chemotherapy.

Typically, in current clinical practice, erlotinib is prescribed to advanced non-small cell lung cancer patients with tumors harboring an EGFR sensitizing mutation, due to its higher likelihood of response rate and lower overall toxicity rate relative to cytotoxic chemotherapy. However, the original U.S. Food and Drug Administration approval was based on response rate and non-small cell lung cancer, regardless of EGFR mutation status. Erlotinib was one of the treatments from the patient cohort. The use of single agent erlotinib in the murine experiment obviated the need to use potentially more confounding regimens to demonstrate the role of the microbiota such as doublet platinum-based chemotherapy or use of a single agent cytotoxic chemotherapy approved in NSCLC (docetaxel) that was not explored in the patient cohort and may have required additional optimal dose finding for these chemotherapeutics. A recent study identified a consortium of 11 commensal bacterial species that were able to induce intestinal IFN-γ-producing CD8 T cells [15]. The investigators demonstrated that this bacterial consortium significantly enhanced efficacy of a checkpoint inhibitor treatment in a syngeneic mouse tumor model. The inventors hypothesized that the

inventor's identified R consortium could similarly activate cells of the immune system, which, in turn, would enhance the susceptibility of cancer cells to treatment outcome. Consequently, the inventors found that the two species enriched in the R group, B. xylanisolvens and B. ovatus, in combination showed a synergistic effect with erlotinib. This effect on tumor progression could be partially mediated by activating the intratumoral mRNA expression of chemokines, which recruits dendritic cells and T cells. This observation is consistent with previous reports that indicate the infiltration of beneficial T cells into the intratumoral microenvironment mediated by specific gut bacteria, resulting in tumor size reduction. The inventors previously revealed that a novel probiotics mixture can suppress hepatocellular carcinoma growth in mice by reducing the frequency of Th17 cells, the main producers of the IL-17 cytokine, in the intestine and their subsequent recruitment to the tumor bed [9], whereas Akkermansia muciniphila was recently identified as being associated with increased intratumoral immune infiltrates into the tumor bed in response to PD-1 blockade therapy [13]. Taken together, the inventors believe that the administration of specific probiotic bacteria could be a potential supplemental treatment in combination with anticancer therapies for a better treatment outcome.

The global cancer burden has risen dramatically making it an urgent need to develop novel therapies and predict which treatment will offer the most benefit to a cancer patient. Here, the inventors analyzed the gut microbiota in a cohort that included eight different cancer types using metagenomic sequencing and found out that gut micro biome signatures at baseline accurately predict cancer treatment outcome. Furthermore, by evaluating the role of the gut microbiota for the first time in a heterogeneous patient cohort with various types of cancer and anticancer treatments, the inventors have demonstrated a more global finding of a microbiota signature that is independent of cancer type and heterogeneity. Moreover, oral gavage of specific gut microbes significantly increased the effect of chemotherapy in mice, reducing the tumor volume by 46% compared to the control.

The gut microbiota has the potential to influence the efficacy of cancer therapy. Here, the inventors investigated the contribution of the intestinal microbiome on treatment outcomes in a heterogeneous cohort that included multiple cancer types to identify

microbes with a global impact on immune response. Human gut metagenomic analysis revealed that responder patients had significantly higher microbial diversity and different microbiota compositions compared to non-responders. A machine-learning model was developed and validated in an independent cohort to predict treatment outcomes based on gut microbiota composition and functional repertoires of responders and non-responders. Specific species, Bacteroides ovatus and Bacteroides xylanisolvens, were positively correlated with treatment outcomes. Oral gavage of these responder bacteria significantly increased the efficacy of erlotinib and induced the expression of CXCL9 and IFN-γ in a murine lung cancer model. These data suggest a predictable impact of specific constituents of the microbiota on tumor growth and cancer treatment outcomes with implications for both prognosis and therapy.

The high accuracy of the inventor's prediction models indicates that the initial condition of the gut microbiota could be a potential predictive tool for response to anticancer treatments. Furthermore, the performance comparisons of the inventor's models suggest that combining the features of both taxa and functions improves the prediction accuracy.

The present invention shall now be further described in the following examples with reference to the accompanying figures, nevertheless, without being limited thereto. For the purposes of the present invention, all references as cited herein shall be incorporated by reference in their entireties. In the Figures,

Figure 1 shows the taxonomic analysis of intestinal microbiota of cancer patients. a Sample collection scheme and dendrogram based on Bray-Curtis dissimilarity. b Alpha diversity (Shannon index) of the gut microbiota in responders (R) and non-responders (NR). c Non-metric multidimensional scaling (NMDS) plot of R and NR in human cancer samples based on the gut microbial compositions using Bray-Curtis dissimilarities (ANOSIM $p = 0.0001$). Intrapatient samples are linked to each other. d NMDS plot of R, NR, and HMP samples based on the gut microbial compositions at the species level using Bray-Curtis dissimilarities (ANOSIM $p = 0.0001$). e Phylogenetic composition of cancer samples at the phylum level. f Firmicutes/Bacteroidetes (F/B) ratio of cancer samples. g Heatmap of differentially abundant species detected in the comparison of R and NR (FDR $p < 0.05$, Wilcoxon rank-sum test). R-associated and

NR-associated bacteria validated in mouse model are shown in light gray and darker gray asterisks, respectively

Figure 2 shows bacterial species co-abundance networks. a Network in responders. b Network in non-responders. Each node represents a species and edges correspond to significant species-species associations as inferred by BAnOCC [26]. The size of each node is proportional to the mean relative abundance. The 95% credible interval criteria were used to assess significance, and estimated correlations were then filtered with the correlation coefficient ≥ 0.4. The shown subnetworks were made by extracting the edges that are connected with B. ovatus, B. xylanisolvens, C. symbiosum, and R. gnavus, which are further highlighted.

Figure 3 shows the functional profiles of intestinal microbiota of cancer patients. a NMDS plot of cancer samples based on KEGG pathway abundances using Bray-Curtis dissimilarities (ANOSIM $p = 0.0299$). b Differentially abundant KEGG pathways (FDR $p < 0.1$, Wilcoxon rank-sum test) detected in the comparison of responders (R) and non-responders (NR). c CAZy class comparison between R and NR. $^{*}p < 0.1$, $^{**}p < 0.05$. d Performance of the C5.0 decision tree models in classifying R and NR.

Figure 4 shows the Increased anti-tumor efficacy of chemotherapy in the presence of B. ovatus and B. xylanisolvens. a Experimental design: male 6-week C57BL6/N mice (n = 5–8) were treated with antibiotic cocktail in drinking water for 1 week before bacterial oral gavage. Control PBS, B. ovatus and B. xylanisolvens, and C. symbiosum and R. gnavus were orally gavaged into mice 1 week prior to tumor cell inoculation. A total of 107 Lewis lung cancer cells in 200 µl PBS were subcutaneously injected into the mice to induce tumor formation. Mice were treated with erlotinib (60 mg/kg body weight) once the tumor size reached approximately 250–500mm3. Time in days is relative to tumor cells injection. b Tumor size measurement at day 14. c Tumor growth curve after Lewis lung carcinoma cell inoculation. Dark dots indicate the application of erlotinib. d, e CRL5883 bronchoalveolar carcinoma cell line was cultured for 72 h in the presence of erlotinib (d) or drug-free (e) supernatants from R (B. xylanisolvens and B. ovatus) or NR (R. gnavus and C. symbiosum) bacteria species. d Non-linear regression curves showing cell viability as percentage of cell control viability. Bacterial supernatants had

n = 4, GAM control had n = 2, and cell control had n = 10. e Cell viability is presented as percentage of cell control viability. Colored circles show individual data points. Outliers were identified and removed by the ROUT method (Q = 0.1%). Supernatants had n = 3–4 and cell control had n = 16. All data are mean ± SEM. Significant differences were identified via unpaired t test (*p < 0.05, **p < 0.005). f, g Tumor expressions of chemokines involved in the recruitment of T cells (f), myeloid cells, and cytotoxic T cells (g) by real-time PCR (normalized against GAPDH). Data are presented as mean ± SEM. *p < 0.05, **p < 0.01, ***p < 0.001.

Examples

Methods

Cancer cohort and treatment outcomes

The 26 cancer patients signed informed consent forms and were enrolled at the Western Regional Medical Center, Goodyear, AZ, after Western Institutional Review Board approval (WIRB #20140271). The patients were diagnosed with eight types of cancers and received either chemotherapy or a combination of chemo- and immunotherapy (Table S1). The 26 patients were classified into responders (n = 16) and non-responders (n = 10) based on their responses to anticancer treatment as defined by RECIST 1.1 [24] and irRECIST [25]. Furthermore, seven more additional cancer patients were recruited and metagenomics sequencing were performed to serve as an independent validation dataset (baseline samples from R = 5, NR = 2) to test the general applicability of the prediction model. The taxonomic profiles for a total of 138 stool samples from the Human Microbiome Project (HMP), as provided by MetaPhlAn2 [39] (http://segatalab.cibio.unitn.it/tools/metaphlan2/), were used as a healthy control in the taxa comparison.

Metagenomic library construction and sequencing

To examine the gut microbiome of the inventor's cancer cohort, 71 fecal samples were collected longitudinally from 26 patients before and after treatments. Bacterial DNA was isolated from the fecal samples for shotgun metagenomic sequencing. Library preparation (using KAPA Hyper Prep Kit KR0961-V1.14) and Illumina sequencing were done at the University of Hong Kong, Centre for Genomic Sciences (HKU, CGS), using Illumina HiSeq 1500 with PE100 at an average depth of 6.1 Gbp (s.d. 1.3 Gbp per

sample) (deposited in the European Nucleotide Archive with accession number PRJNA494824).

Quality control and taxonomic profiling

The sequenced reads were processed with quality control to remove the adapter regions, low quality reads/bases using fqc.pl with default settings (https://github.om/TingtZHENG/VirMiner/tree/master/scripts/PipelineForQC) [40], and human DNA contaminations (bwa (version 0.7.4-r385) mem against human reference genome ucsc.hg19), following the previously described steps [9, 41]. Approximately 85% of the reads on average remained after the quality control and were used in downstream analyses. The high-quality reads were taxonomically profiled at different taxonomic levels using MetaPhlAn2 [39] with default settings, generating taxonomic relative abundances (total sum scaling normalization). The differentially abundant taxa were identified by the Wilcoxon rank-sum test, and the statistical significance was adjusted for multiple testing using FDR correction with the cutoff adjusted p value < 0.05, unless otherwise stated. ConStrains was utilized for strain level analysis with default settings [42].

Microbial community diversity analysis

The alpha diversity (Shannon index) of each sample was calculated with R package VEGAN [43] (v2.5.3) on the relative abundance of species. Species richness for all samples was estimated based on rarefied data. Beta diversities (Bray-Curtis dissimilarities) among samples were calculated with VEGAN based on the relative abundance of species. To test the difference in the microbial composition between two or more groups, ANOSIM (analysis of similarities) was employed based on the Bray-Curtis dissimilarity.

Species co-abundance network inference

For species co-abundance network reconstruction, the OTU relative abundance table was split into responder and non-responder samples, and they were processed independently with BAnOCC [26] for co-abundance network inference with 5000 iterations. A correlation estimate is considered significant if the corresponding 95% credible interval excludes zero. The estimated correlations were then filtered with the

absolute values of correlation coefficients ≥ 0.4. The co-abundance network was visualized by Cytoscape 3.6.1. For visualizing Fig. 2, the subsets of networks were taken by extracting the edges that are connected with B. ovatus, B. xylanisolvens, C. symbiosum, and R. gnavus.

De novo assembly and functional annotation

The high-quality reads after quality control were assembled using IDBA-UD [44] with k-mer size ranging from 20 to 100 bp. The coding DNA sequence (CDS) regions were predicted using MetaGeneMark [45] with the default parameters. The predicted peptide sequences were mapped to the KOBAS database [46] and dbCAN database [47] using DIAMOND [48] with the default parameters for KEGG (through KOBAS 2.0 annotate program) and CAZy annotation, respectively. The protein sequences were also assigned to the functional category of COG [49] using NCBI RPS-BLAST with default parameters. The abundance of genes was quantified in an RPKM (Reads Per Kilobase of transcript per Million mapped reads)-like manner using custom Perl scripts. Bray-Curtis dissimilarity calculated with VEGAN (v2.5.3) based on KEGG Orthologs was used to evaluate functional diversity between samples. KEGG pathway and module abundances were estimated by summing up the abundances of all genes present in the corresponding pathway or module (KEGG database accessed in December 2017).

Classifier model

Fivefold cross-validation was performed on a C5.0 decision tree model (R 3.3.0, C50 0.1.1 package), using as predictors the differentially abundant species (FDR $p < 0.05$) and pathways (FDR $p < 0.05$) that were identified by comparing responders and non-responders. As a reference, the inventors cited a study that used preselected features to build a classification model to predict the therapy response of inflammatory bowel disease [31].

Bacterial strains and culture conditions

Bacteroides ovatus (ATCC 8483), Bacteroides xylanisolvens (DSM-18836), Ruminococcus gnavus (ATCC29149), and Clostridium symbiosum (ATCC 14940) were grown at 37 °C under anaerobic conditions (Anaerobic gas mixture, 95% N2 and 5% H2) in pre-reduced GAM (Gifu anaerobic media; Nissui Pharmaceutical Co. Ltd.)

broth for liquid culture or broth supplemented with agar (Gifu anaerobic media agar; Nissui Pharmaceutical Co.Ltd.) for growth on plates.

Cell lines and culture conditions

The bronchoalveolar carcinoma cell line NCI-H1650 (ATCC CRL-5883) was cultured at 37 °C under 5% CO_2 in Roswell Park Memorial Institute (RPMI) 1640 medium (ATCC modification; Thermo Fisher Scientific) supplemented with 10% Fetal Bovine Serum (FBS; Himedialabs) and antibiotics (~ 5000 units penicillin, 5mg streptomycin, and 10 mg neomycin/mL). The cell line was maintained from frozen stock and allowed to grow for a minimum of 3 days before being used in the supernatant assays. Passage number was kept below 10. Lewis lung cancer cells (LLC) were cultured at 37 °C under 5% CO_2 in Dulbecco's modified Eagle medium (DMEM; Life technologies) supplemented with 10% FBS and antibiotics (100 U penicillin, 0.1 mg streptomycin, and 0.25 µg/ml amphotericin B).

Supernatant exposure assay

Bacterial strains growing overnight in GAM broth were sub-cultured 1:50 in fresh GAM broth and grown for 24 h. Bacterial cultures were spun down at 11,000×g for 2 min and the supernatant carefully removed without disturbing the pellet. The supernatants were filtered through a 0.2-µM syringe filter to remove any remaining bacteria in suspension. For the erlotinib supernatant assay, 15 ml conical Greiner tubes (Sigma-Aldrich) were filled with GAM broth supplemented with an erlotinib (erlotinib hydrochloride dissolved in DMSO; Sigma-Aldrich) gradient ranging from 0 to 100 µM. The tubes were inoculated 1:50 with sub-cultured bacteria growing for 24 h. The bacterial culture was exposed to erlotinib for 24 h, before following the same procedure for supernatant preparation as described above. Supernatants were stored at − 20 °C until being un-thawed and homogenized by vortexing for the subsequent assays. Wells of a black, clear bottom 96-well plate were seeded with NCI-H1650 cells at a density of 5 × 103 in either 90 µl or 50 µl of complete growth medium with antibiotics for the erlotinib or drug-free supernatant assays, respectively. Cells were allowed to attach for 1 day. The following day, respective bacterial supernatants were added to the attached cells at a ratio of 1:10 or 1:1 for the erlotinib or drug-free supernatant assays, respectively. Dilution of supernatants resulted in final erlotinib concentrations of 0–10

μM and final supernatant dilutions of 0–40% in the respective wells. Cell control wells received either DMSO or PBS for the erlotinib or supernatant assay, respectively. GAM control wells were bacteria free and otherwise handled the same as bacterial supernatants. In both assays, plates were incubated for 72 h at 37 °C under 5% CO_2. Viability was assessed by addition of 5% of a resazurin-based cell viability reagent (alamarBlue; Thermo Fisher Scientific) and further incubation for approximately 18 h. The reducing capability of viable cells was assessed by measuring fluorescence at 530EX nm/590EM nm in a Synergy H1 microplate reader (BioTek). Higher fluorescence signal indicated higher cell viability.

Animal studies

Six-week old C57BL6/N mice were fed on a normal chow diet ad libitum. Mice were treated with a cocktail of antibiotics (ampicillin 0.3 g/L, neomycin 0.3 g/L, metronidazole 0.3 g/L, and vancomycin 0.15 g/L) in drinking water for 1 week before oral gavage of bacterial species. Control PBS, responder-enriched species (B. ovatus and B. xylanisolvens) and non-responder-enriched species (C. symbiosum and R. gnavus) were orally gavaged into mice respectively 1 week prior to the inoculation of the tumor cell line and daily throughout the entire experiments. To induce tumor formation, 107 Lewis lung cancer cells in 200 μl PBS were subcutaneously injected into the mice. Mice were treated with or without erlotinib (60 mg/kg body weight) once the tumor size reached approximately 250–500mm3. Tumor growth was assessed using a caliper, and tumor size was estimated by using the following formula: tumor size = length × width × width/2. All animal experiments were approved by the Committee on the Use of Live Animals for Teaching and Research of the University of Hong Kong.

Gut colonization with responder-enriched species and non-responder-enriched species

B. ovatus, B. xylanisolvens, C. symbiosum, and R. gnavus were cultured anaerobically in GAM (Gifu anaerobic medium) broth. Colonization of antibiotic-pretreated C57BL/6 N mice was performed by oral gavage with 200 μl of suspension containing 5×10^9 bacteria. The efficacy of colonization was confirmed by detecting the fecal content of bacterial species on day 14 (at the end of the experimental stage), based on pre-built standard curves and normalization by the gram of feces. Fecal DNA was extracted with

the QIAamp DNA stool mini kit (Qiagen) and subjected to PCR amplification targeting different bacterial species. Primers for B. ovatus and B. xylanisolvens were as follows: forward: GGTGTCGGCTTAAGTGCCAT (SEQ ID NO: 1); reverse: CGGACGTAAGGGCCGTGC (SEQ ID NO: 2). Primers for C. symbiosum and R. gnavus were as follows: forward: CGGTACCTGACTAAGAAGC (SEQ ID NO: 3); reverse: AGTTTCATTCTTGCGAACG (SEQ ID NO: 4).

Quantitative real-time PCR

Tumors were frozen in liquid nitrogen immediately after harvest, and total RNA was extracted with RNAiso Plus (Takara) and reverse transcribed into complementary DNA with a primeScript RT reagent kit (Takara). Quantitative real-time PCR was performed by using SYBR Premix Ex Taq (Takara) with specific primers on a StepOnePlus Real-798 time PCR system (Applied Biosystems). Primers for CXCL9 were as follows: forward: GGAGTTCGAGGAACCCTAGTG (SEQ ID NO: 5); reverse: GGGATTTGTAGTGGATCGTGC (SEQ ID NO: 6). Primers for CXCL10 were as follows: forward: CCAAGTGCTGCCGTCATTTTC (SEQ ID NO: 7); reverse: TCCCTATGGCCCTCATTCTCA (SEQ ID NO: 8). Primers for IFN-γ were as follows: forward: ATGAACGCTACACACTGCATC (SEQ ID NO: 9); reverse: CCATCCTTTTGCCAGTTCCTC (SEQ ID NO: 10). Primers for CCL20 were as follows: forward: ACTGTTGCCTCTCGTACATACA (SEQ ID NO: 11); reverse: GAGGAGGTTCACAGCCCTTTT (SEQ ID NO: 12). Primers for granzyme B were as follows: forward: TCTCGACCCTACATGGCCTTA (SEQ ID NO: 13); reverse: TCCTGTTCTTTGATGTTGTGGG (SEQ ID NO: 14). Primers for MCP-1 were as follows: forward: CCACTCACCTGCTGCTACTCA (SEQ ID NO: 15); reverse: TGGTGATCCTCTTGTAGCTCTCC (SEQ ID NO: 16). Primers for SDF-1 were as follows: forward: TGCATCAGTGACGGTAAACCA (SEQ ID NO: 17); reverse: CACAGTTTGGAGTGTTGAGGAT (SEQ ID NO: 18).

Statistical analysis

'The significance of the differences between groups was analyzed using the Wilcoxon rank-sum test and ANOSIM with R. A p value < 0.05 (5% level of probability) was considered to be significant and denoted as follows: $*p < 0.05$, $**p < 0.01$, $***p < 0.001$, and $****p < 0.0001$. In in vitro assays, cell viability percentage was calculated as

percentage of average viability from cell control wells. Outliers were identified with the ROUT method using a strict threshold of Q = 0.1%. Identified outliers were removed for subsequent statistical analysis. For non-linear regression curves, differences in IC50 values were determined with the extra sum-of-squares F-test. Significant differences between bacterial and GAM control wells were determined via an unpaired t test and a false discovery rate approach using the two-stage linear step-up procedure of Benjamini, Krieger, and Yekutieli, with a false discovery rate (Q) of 1%. Testing conditions were analyzed individually, without assuming a consistent SD. Statistical analysis in vitro was performed with GraphPad Prism (version 8.0.0 for Mac, GraphPad Software, San Diego, CA, USA, www.graphpad.com).

Results

Limited impact of cancer therapy on individual gut microbiota

The inventor's cohort was comprised of 26 cancer patients of various cancer types, treated either with cytotoxic or targeted chemotherapy (n = 15) or a combination of cytotoxic or targeted chemotherapy with immunotherapy (n = 11). The inventors collected 71 fecal samples from the 26 patients at four different time points (B1: baseline, B2: base-line at least 24 h after B1, T1: end of cycle 1 of treatment ± 5 days, T2: end of cycle 2 of treatment ± 5 days). All the samples were further combined into two groups, namely baseline (n = 31, comprised of B1 and B2) and treatment (n = 40, comprised of T1 and T2).

The inventors assessed the structure of the gut microbiome in all available samples (n = 71) via shotgun metagenomic sequencing, generating 6.1 Gbp of sequencing data on average (s.d. 1.3 Gbp per sample). The taxonomic profiling revealed that Bacteroidetes (44.51% on average) and Firmicutes (44.04%) were the most abundant phyla across all samples, followed by Proteobacteria (4.09%) and Verrucomicrobia (3.53%). To test whether the gut microbiota compositions of patients with different cancer types share similar profiles, the inventors investigated the cancer type-specific microbiome signatures. The 26 patients were classified according to their primary site of tumors: lung (n = 8), breast (n = 7), colon (n = 2), rectal (n = 2), pancreatic (n = 2), ovarian (n = 2), prostate (n = 2), and blood (n = 1). The dendrogram clustering based on taxonomic profiles showed that interpatient samples with the same cancer type did not necessarily

cluster together, while the intrapatient samples tend to cluster closely with relatively minimal impact from the anticancer treatment (Fig. 1a) as previously reported [16–18]. Subsequently, the inventors further compared the gut microbiota communities of baseline versus treatment to investigate any global patterns of anticancer therapies on gut microbial compositions. The alpha diversity comparison indicated that the baseline and treatment samples had similar levels of diversity ($p = 0.265$, Wilcoxon rank-sum test). Likewise, the ordination plot based on the beta diversity (Bray-Curtis dissimilarity) indicated no difference between baseline and treatment ($p = 0.364$, ANOSIM), suggesting that anticancer therapy may not introduce drastic changes to the overall structure of the gut microbial community. Moreover, no differentially abundant taxa, functional pathways, or modules could be identified by comparing baseline versus treatment samples in the inventor's data set.

Given the well-reported stability and resilience of individual signatures of human gut microbiota [17, 18], as well as the limited and non-significant effects of cancer types and anticancer treatments observed in the inventor's cohort, the inventors combined the 71 samples and, similarly to microbiome meta-analysis studies [15, 19], performed a comparison with publicly available data to evaluate whether the cancer patients present distinct gut microbial profiles. The inventors used, in the comparison, the gut microbiome samples of 138 healthy individuals from the Human Microbiome Project (HMP) [16], which, as the inventor's cohort, also consists of US subjects. The beta diversity comparison of cancer and HMP microbiome samples revealed that the two cohorts had significantly different species compositions of intestinal bacteria ($p = 0.0001$, ANO SIM), while there was no significant difference on alpha diversity at the species level between the two cohorts ($p = 0.07373$, Wilcoxon rank-sum test). In HMP, the mean abundance of the phylum Bacteroidetes across all HMP stool samples was 74.96%, followed by 22.07% of Firmicutes, indicating that the cancer cohort had a significantly higher Firmicutes/Bacteroidetes (F/B) ratio ($p = 2.461e{-}13$, Wilcoxon rank-sum test). Compared with healthy individuals, a higher F/B ratio has also been observed in patients with irritable bowel syndrome (IBS), hypertension, autism, and chronic fatigue syndrome in case control studies [20–23]. Taken together, these comparisons above suggest that cancer treatments may not significantly disrupt the

patients' individual signatures of gut microbiota; however, the cancer patients have distinct gut microbiota features compared to the healthy cohort.

Responders have higher ecological diversity than non-responders

To evaluate the association between the microbial community and treatment outcome, the inventors grouped the patients based on their response to treatment (responders: R, n = 16; non-responders: NR, n = 10). The classification of patients was based on the Response Evaluation Criteria in Solid Tumors (RECIST 1.1) [24] or immune-related response criteria (iRECIST) [25]. The R group achieved a favorable response (complete or partial response or stable disease status) as their best response, while the NR group showed disease progression as their best response to the administered systemic treatment. The patients in the two groups were similar in terms of stage of cancer, sex, age, and therapy type. A comparison of the gut microbiome of these two groups revealed that R had higher alpha diversity than NR ($p = 0.003$, Wilcoxon rank-sum test, combined samples from baseline and treatment) (Fig. 1b). It led to the same conclusion when using just treatment samples ($p = 0.008$, Wilcoxon rank-sum test), though only showed trends when focusing on the baseline samples. Despite the difference in alpha diversity, R and NR showed similar levels of species richness (Chao1) ($p = 0.674$, Wilcoxon rank-sum test). Furthermore, the ordination plot based on Bray-Curtis dissimilarities revealed distinct intestinal microbial compositions at the species level between R and NR ($p = 0.0001$, ANOSIM) (Fig. 1c). Unweighted and weighted UniFrac distances were consistent with this result ($p = 0.0001$ and $p = 0.0006$). Interestingly, the inventors also observed a clear gradation of NR, R, and healthy subjects (HMP) ($p = 0.0001$, ANOSIM) (Fig. 1d), with the majority of R samples overlapping with the HMP subjects, whereas NR samples were clearly distinct from those of the healthy subjects. This gradation suggests that the patients in R group have relatively more similar gut microbiota profiles to the healthy individuals.

No significant differences of alpha diversity between the baseline and treatment were observed either in R or NR ($p = 0.3254$ and $p = 0.616$ for R and NR, respectively, Wilcoxon rank-sum test) (Fig. 1b). Furthermore, the treatment impact on the gut microbiota of the two groups (R and NR) was also measured based on the Bray-Curtis dissimilarities between intrapatient baseline and treatment using the relative abundances

of species or strains. The comparison showed no difference between R and NR in terms of the therapy impact on their gut microbial compositions at the community level ($p = 0.216$ and $p = 0.204$ for species and strains, respectively, Wilcoxon rank-sum test).

Identification of specific taxa related to cancer treatment response

The inventors next searched for differentially abundant taxa in the gut microbiome of R versus NR. The enrichment analysis revealed that, at the phylum level, Bacteroidetes was enriched in R in the treatment samples (FDR $p = 0.031$, Wilcoxon rank-sum test) but not in the baseline samples (FDR $p = 0.540$, Wilcoxon rank-sum test) (Fig. 1e). Additionally, comparing Firmicutes/Bacteroidetes (F/B) ratios, the inventors noticed that NR showed a significantly higher ratio than R ($p = 0.037$, Wilcoxon rank-sum test) (Fig. 1f) and healthy individuals from the HMP (138 subjects, $p = 1.617e{-}09$, Wilcoxon rank-sum test), which is in agreement with the findings described above regarding the microbiome profiles of healthy individuals and cancer patients.

In the comparison between R and NR, 31 differentially abundant species (FDR $p < 0.05$, Wilcoxon rank-sum test) were identified. As shown in Fig. 1g, 22 and 9 species were R-enriched and NR-enriched, respectively. Bacteroides xylanisolvens, Bacteroides ovatus, Prevotella copri, and seven Alistipes species, among others, were found to be significantly enriched in R compared to NR (FDR $p < 0.05$, Wilcoxon rank-sum test) (Fig. 1g). The inventors found that ~ 73% (16/22) of these species are classified at the phylum level as Bacteroidetes. In contrast, all 9 NR-enriched species, including Clostridium symbiosum and Ruminococcus gnavus, were classified as Firmicutes at the phylum level.

Next, the inventors reconstructed the species co-abundance networks separately for R and NR using BAnOCC [26]. The R network showed that B. xylanisolvens was correlated with other Bacteroidetes species and Proteobacteria, while this species did not show any significant associations in the NR network (Fig. 2a). On the other hand, the NR network shows that C. symbiosum and R. gnavus have a positive association with each other and both have a negative association with one of the R-associated species B. ovatus (Fig. 2b). Furthermore, in the NR network, both C. symbiosum and R. gnavus retained their positive interactions mostly within Firmicutes with only one exception (a positive interaction between C. symbiosum and Klebsiella pneumoniae),

whereas their interactions with Bacteroidetes species were all negative. Altogether, it is suggested that the high abundances of C. symbiosum and R. gnavus in NR might promote the dominance of Firmicutes and impede Bacteroidetes by their intra-phylum positive associations along with the negative associations with Bacteroidetes species including B. ovatus. This observation is in line with the aforementioned high Firmicutes/Bacteroidetes (F/B) ratio in NR (Fig. 1f). Lastly, R. gnavus, as well as other Firmicutes species, were positively correlated with the F/B ratio ($r = 0.5665$, $p = 0.0021$, Pearson correlation).

Anabolism enriched in responders' and catabolism in nonresponders' microbial communities

The Bray-Curtis dissimilarities based on 146 annotated KEGG pathway abundances illustrate the marginally separate clusters of R and NR ($p = 0.0299$, ANOSIM) (Fig. 3a). The KEGG pathway enrichment analysis of the metagenomic data shows that the majority of 32 pathways overrepresented in NR were catabolic pathways including ABC transporter, phosphotransferase system (PTS), carbohydrate metabolism pathways, and xenobiotic degradation pathways (FDR $p < 0.1$, Wilcoxon rank-sum test) (Fig. 3b), whereas anabolic pathways were in contrast overrepresented in R. This tendency is also consistent with the recently published study of anti-PD-1 immunotherapy in melanoma patients, which also reported that NR patients' intestinal microbial communities had more enriched catabolic pathways compared to R [12]. Additionally, the Carbohydrate-Active enZymes (CAZy) annotation and the analysis of Clusters of Orthologous Groups (COG) supported the overrepresentation of catabolic functions in NR; three CAZy classes, "glycoside hydrolases," "carbohydrate-binding modules," and "auxiliary activities" were overrepresented in NR (FDR $p < 0.1$, Wilcoxon rank-sum test), whereas no CAZy classes were significantly enriched in R (FDR $p > 0.1$, Wilcoxon rank-sum test) (Fig. 3c); NR had six enriched COG classes including "carbohydrate transport and metabolism" and "amino acid transport and metabolism" (FDR $p < 0.1$, Wilcoxon rank-sum test). Although anabolic functions such as "valine, leucine, and isoleucine biosynthesis" and "unsaturated fatty acids biosynthesis" were exceptionally enriched in NR, these BCAA microbial metabolites have been found to be positively associated with cancers and related to tumor metabolic needs [27]. Likewise, unsaturated fatty acids have been suggested to be involved in the

metastasis and stemness of certain cancers [28]. Furthermore, previous case-control gut microbiome studies reported that enrichment of ABC transporter and PTS in microbial communities are associated with inflammation, which has been shown to promote tumor growth in cancer patients [29].

In contrast, the pathway enrichment analysis revealed that the most significantly enriched pathways in R were biosynthetic pathways of metabolites including flavonoid, zeatin, and secondary bile acids (FDR $p < 0.1$, Wilcoxon rank-sum test) (Fig. 3b). The comparison of KEGG modules revealed that in R, 20 modules including the biosynthesis of lipopolysaccharide (LPS) were enriched (FDR $p < 0.1$, Wilcoxon rank-sum test). Bacterial LPS is known to induce the differentiation of Th17 cells [30].

Initial microbiota composition and functionality predicts response to treatment

After identifying differences in intestinal microbial composition between R and NR in the inventor's cohort, the inventors examined whether statistical modeling would enable prediction of treatment response based on the initial gut microbial status of the cancer patients. In addition to the anticancer therapy response, a recent study showed that the anti-integrin therapy response of inflammatory bowel disease patients could be predicted using the information of initial conditions of their preselected gut microbiota features based on a deep neural network [31]. However, to the best of the inventor's knowledge, there are no models used to predict the anticancer treatment response that covers broad types of cancer and treatments. The inventors built a classification model based on decision tree using the features of baseline samples with a fivefold cross-validation.

The inventors used the relative abundances at the baseline of 31 differentially abundant species between R and NR (Fig. 1g) and the baseline RPKM of the differentially abundant KEGG pathways (Fig. 3b). The model performance was evaluated with an area under the curve (AUC) of receiver operating characteristic (ROC). Using the initial relative abundance of differentially abundant species solely, the performance was the lowest (AUC = 0.652) (Fig. 3d). The prediction performance was significantly improved by using the RPKM of differentially abundant KEGG pathways solely (AUC = 0.707). However, the model incorporating data on both species and pathways showed

the best performance (AUC = 0.895), indicating the power of shotgun metagenomics for predicting host phenotypes. To further test the general applicability of the model, the inventors recruited additional cancer patients and performed metagenomics sequencing in seven more patients (baseline samples from R = 5, NR = 2) to serve as an independent validation dataset. Using the initial relative abundance of differentially abundant species and the RPKM of differentially abundant KEGG pathways, the inventors could achieve an AUC = 0.75.

Oral gavage of responder bacteria reduces tumor size during erlotinib treatment in mice

To test if there is a causal effect of the R and NR bacteria on treatment outcomes, the inventors tested their impact on tumor growth in a murine lung cancer model [32]. As examples of the R-enriched bacteria, B. ovatus and B. xylanisolvens were chosen due to their relatively high significance in the species enrichment analysis described above (Fig. 1g). In addition, the inventors selected C. symbiosum and R. gnavus due to their relatively high prevalence (63% and 67% for C. symbiosum and R. gnavus, respectively) in NR samples. The inventors selected Lewis lung carcinoma cells and erlotinib to test in the murine model, as the majority of the inventor's patient cohort suffered from forms of lung cancer, and erlotinib is a commonly used drug for non-small cell lung cancers [33]. The inventors introduced either R (B. ovatus and B. xylanisolvens) or NR bacteria (C. symbiosum and R. gnavus) by daily oral gavage in antibiotic-pretreated mice (Fig. 4a). One week later, Lewis lung carcinoma cells were subcutaneously inoculated into these C57BL/6 N mice to induce tumor formation. When the tumor size reached approximately 250–500mm3, erlotinib was administered. Erlotinib significantly inhibited the tumor growth by 56% compared to the control group (PBS + DMSO) after 1 week (Fig. 4b and Fig. 4c). The R-enriched species alone reduced (by 20%) the tumor progression in mice compared to the control, but the difference was not statistically significant ($p = 0.1949$, Wilcoxon rank-sum test). However, the presence of B. ovatus and B. xylanisolvens led to additional significant reductions in tumor size in the erlotinib-treated mice (Fig. 4b). On day 14, the average tumor volume in erlotinib-treated mice colonized with the R-enriched species (R + erlotinib) was significantly smaller (46%) than that of the erlotinib-treated group (PBS + erlotinib) ($p = 0.032$, Wilcoxon rank-sum test), as well as that of the NR + erlotinib

group (Fig. 4b and Fig. 4c) (p=0.032, Wilcoxon rank-sum test). This demonstrates that simultaneous administration of B. ovatus and B. xylanisolvens increases the efficacy of erlotinib, suggesting that these R-enriched species could have a positive impact on therapeutic outcome in cancer. Interestingly, by comparing the tumor sizes among groups on day 10, the NR + erlotinib group had a significantly larger tumor size (87%) compared to that of R + erlotinib (p = 0.0317, Wilcoxon rank-sum test), which was commensurate with the control group without erlotinib (PBS + DMSO and R+DMSO) (Fig. 4c). This suggests the potential contribution of C. symbiosum and R. gnavus on treatment resistance.

To assess if there was a direct impact of the R bacteria on drug efficacy, the inventors grew the R and NR bacteria in GAM media containing erlotinib. Subsequent addition of this spent media to the bronchoalveolar carcinoma cell line NCI-H1650 did not result in significant changes in the IC50 of erlotinib suggesting a limited direct impact of the R bacteria on erlotinib (Fig. 4d). To further investigate if metabolites produced by R and NR bacteria could directly affect the growth of cancer cells, the inventors tested different dilutions of spent media from the R and NR bacteria on NCI-H1650 cell line viability. The inventors observed that increasing amounts of spent media affected cancer cell line viability. The viability effects were species-specific and varied within the R and NR groups (Fig. 4e). These in vitro data suggest that bacterial effects on treatment outcome might be caused by multiple rather than single species acting in a consortium or that the beneficial effects depend on the host response to the specific bacteria. To explore the mechanisms of how R-enriched bacteria increase the efficacy of chemotherapy, the inventors examined the tumor expression of different chemokines involved in tumor progression using real-time PCR. Chemokines serve as attractant cytokines for different immune cells to modulate tumor growth through immunoediting. The inventors found a significant increase in the expression of the chemokine (C-X-C motif) ligand 9 (CXCL9) and interferon gamma (IFN-γ) in the tumors of erlotinib-treated mice colonized with R-enriched species (R + erlotinib) compared to that of the control group (PBS + DMSO). CXCL10 expression in tumors also exhibited an increased trend in erlotinib-treated mice colonized with R-enriched species (R + erlotinib) (Fig. 4f). These molecules, which are involved in the recruitment of T cells, are negatively associated with tumor progression [34, 35].

Importantly, such alterations were observed in neither the R-enriched-treated group (R + DMSO) nor the erlotinib-treated group (PBS + erlotinib), suggesting that the presence of R-enriched bacteria and erlotinib has a synergistic effect in modulating the immune responses of T cells in tumors. The inventors did not observe such a synergistic effect in the expression of granzyme B, which is a serine protease in the granules of cytotoxic T cells (Fig. 4g). Furthermore, the levels of two chemokines, monocyte chemoattractant protein-1 (MCP-1) and stromal derived factor-1 (SDF-1), which are involved in the recruitment of myeloid cells, were comparable among these different groups (Fig. 4g). These findings suggest that the enhancement of chemo therapy efficacy by R-enriched bacteria may be achieved by synergistically upregulating the expression of chemokines involved in the recruitment of T cells.

Literature as cited

1. World Health Organization (2017).

2. Emens LA, Middleton G. The interplay of immunotherapy and chemotherapy: harnessing potential synergies. Cancer Immunol Res. 2015;3: 436–43.

3. Zitvogel L, Ma Y, Raoult D, Kroemer G, Gajewski TF. The microbiome in cancer immunotherapy: diagnostic tools and therapeutic strategies. Science. 2018;359:1366–70.

4. Pouncey AL, Scott AJ, Alexander JL, Marchesi J, Kinross J. Gut microbiota, chemotherapy and the host: the influence of the gut microbiota on cancer treatment. Ecancermedicalscience. 2018;12:868.

5. Takasuna K, et al. Involvement of beta-glucuronidase in intestinal microflora in the intestinal toxicity of the antitumor camptothecin derivative irinotecan hydrochloride (CPT-11) in rats. Cancer Res. 1996;56:3752–7.

6. Geller LT, et al. Potential role of intratumor bacteria in mediating tumor resistance to the chemotherapeutic drug gemcitabine. Science. 2017;357: 1156–60.

7. Iida N, et al. Commensal bacteria control cancer response to therapy by modulating the tumor microenvironment. Science. 2013;342:967–70.

8. Viaud S, et al. The intestinal microbiota modulates the anticancer immune effects of cyclophosphamide. Science. 2013;342:971–6.

9. Li J, et al. Probiotics modulated gut microbiota suppresses hepatocellular carcinoma growth in mice. Proc Natl Acad Sci U S A. 2016;113:E1306–15.

10. Sivan A, et al. Commensal Bifidobacterium promotes antitumor immunity and facilitates anti-PD-L1 efficacy. Science. 2015;350:1084–9.

11. Frankel AE, et al. Metagenomic shotgun sequencing and unbiased metabolomic profiling identify specific human gut microbiota and metabolites associated with immune checkpoint therapy efficacy in melanoma patients. Neoplasia. 2017;19:848–55.

12. Gopalakrishnan V, et al. Gut microbiome modulates response to anti-PD-1 immunotherapy in melanoma patients. Science. 2017. https://doi.org/10.1126/science.aan4236.

13. Routy B, et al. Gut microbiome influences efficacy of PD-1-based immunotherapy against epithelial tumors. Science. 2017. https://doi.org/10.1126/science.aan3706.

14. Derosa L, et al. Negative association of antibiotics on clinical activity of immune checkpoint inhibitors in patients with advanced renal cell and non-small-cell lung cancer. Ann Oncol. 2018;29:1437–44.

15. Tanoue T, et al. A defined commensal consortium elicits CD8 T cells and anti-cancer immunity. Nature. 2019;565:600–5.

16. Human C. Microbiome project, structure, function and diversity of the healthy human microbiome. Nature. 2012;486:207–14.

17. Lozupone CA, Stombaugh JI, Gordon JI, Jansson JK, Knight R. Diversity, stability and resilience of the human gut microbiota. Nature. 2012;489:220–30. 973

18. Mehta RS, et al. Stability of the human faecal microbiome in a cohort of adult men. Nat Microbiol. 2018;3:347–55. 975

19. Thomas AM, et al. Metagenomic analysis of colorectal cancer datasets identifies cross-cohort microbial diagnostic signatures and a link with choline degradation. Nat Med. 2019;25:667–78.

20. Nagel R, Traub RJ, Allcock RJ, Kwan MM, Bielefeldt-Ohmann H. Comparison of faecal microbiota in Blastocystis-positive and Blastocystis-negative irritable bowel syndrome patients. Microbiome. 2016;4:47.

21. Yang T, et al. Gut dysbiosis is linked to hypertension. Hypertension. 2015;65: 1331–40.

22. Strati F, et al. New evidences on the altered gut microbiota in autism spectrum disorders. Microbiome. 2017;5:24.

23. Fremont M, Coomans D, Massart S, De Meirleir K. High-throughput 16S rRNA gene sequencing reveals alterations of intestinal microbiota in myalgic encephalomyelitis/chronic fatigue syndrome patients. Anaerobe. 2013;22:50–6.

24. Eisenhauer EA, et al. New response evaluation criteria in solid tumours: revised RECIST guideline (version 1.1). Eur J Cancer. 2009;45:228–47.

25. Weiss GJ, et al. A phase Ib study of pembrolizumab plus chemotherapy in patients with advanced cancer (PembroPlus). Br J Cancer. 2017;117:33–40.

26. Schwager E, Mallick H, Ventz S, Huttenhower C. A Bayesian method for detecting pairwise associations in compositional data. PLoS Comput Biol. 2017;13:e1005852.

27. O'Connell TM. The complex role of branched chain amino acids in diabetes and cancer. Metabolites. 2013;3:931–45.

28. Mukherjee A, Kenny HA, Lengyel E. Unsaturated fatty acids maintain cancer cell stemness. Cell Stem Cell. 2017;20:291–2.

29. Arcidiacono B, et al. Insulin resistance and cancer risk: an overview of the pathogenetic mechanisms. Exp Diabetes Res. 2012;2012:789174.

30. Park JH, Jeong SY, Choi AJ, Kim SJ. Lipopolysaccharide directly stimulates Th17 differentiation in vitro modulating phosphorylation of RelB and NF-kappaB1. Immunol Lett. 2015;165:10–9.

31. Ananthakrishnan AN, et al. Gut microbiome function predicts response to anti-integrin biologic therapy in inflammatory bowel diseases. Cell Host Microbe. 2017;21:603–10 e603.

32. Wang P, et al. Chronopharmacology and mechanism of antitumor effect of erlotinib in Lewis tumor-bearing mice. PLoS One. 2014;9:e101720.

33. Reck M, et al. Erlotinib in advanced non-small cell lung cancer: efficacy and safety findings of the global phase IV Tarceva Lung Cancer Survival Treatment study. J Thorac Oncol. 2010;5:1616–22.

34. Kaplan DH, et al. Demonstration of an interferon gamma-dependent tumor surveillance system in immunocompetent mice. Proc Natl Acad Sci U S A. 1998;95:7556–61.

35. Bronger H, et al. CXCL9 and CXCL10 predict survival and are regulated by cyclooxygenase inhibition in advanced serous ovarian cancer. Br J Cancer. 2016;115:553–63.

36. Korem T, et al. Bread affects clinical parameters and induces gut microbiome-associated personal glycemic responses. Cell Metab. 2017;25: 1243–53 e1245.

37. Magkos F, et al. Effects of moderate and subsequent progressive weight loss on metabolic function and adipose tissue biology in humans with obesity. Cell Metab. 2016;23:591–601.

38. Wu H, et al. Metformin alters the gut microbiome of individuals with treatment-naive type 2 diabetes, contributing to the therapeutic effects of the drug. Nat Med. 2017;23:850–8.

39. Truong DT, et al. MetaPhlAn2 for enhanced metagenomic taxonomic profiling. Nat Methods. 2015;12:902–3.

40. Zheng T, et al. Mining, analyzing, and integrating viral signals from metagenomic data. Microbiome. 2019;7:42.

41. Li J, et al. Antibiotic treatment drives the diversification of the human gut resistome. Genomics Proteomics Bioinformatics. 2019;17:39–51.

42. Luo C, et al. ConStrains identifies microbial strains in metagenomic datasets. Nat Biotechnol. 2015;33:1045–52.

43. Dixon P. VEGAN, a package of R functions for community ecology. J Veg Sci. 2009;14:927–30.

44. Peng Y, Leung HC, Yiu SM, Chin FY. IDBA-UD: a de novo assembler for single-cell and metagenomic sequencing data with highly uneven depth. Bioinformatics. 2012;28:1420–8.

45. Zhu W, Lomsadze A, Borodovsky M. Ab initio gene identification in metagenomic sequences. Nucleic Acids Res. 2010;38:e132.

46. Xie C, et al. KOBAS 2.0: a web server for annotation and identification of enriched pathways and diseases. Nucleic Acids Res. 2011;39:W316–22.

47. Yin Y, et al. dbCAN: a web resource for automated carbohydrate-active enzyme annotation. Nucleic Acids Res. 2012;40:W445–51.

48. Buchfink B, Xie C, Huson DH. Fast and sensitive protein alignment using DIAMOND. Nat Methods. 2015;12:59–60.

49. Tatusov RL, Koonin EV, Lipman DJ. A genomic perspective on protein families. Science. 1997;278:631–7.

Claims

1. A method for prognosing a response to a cancer therapy in a human patient, comprising the steps of
a) detecting the alpha diversity of the gut microbiome in a sample obtained from said human patient, and
b) prognosing the response to cancer therapy in said human patient,
wherein a higher alpha diversity of the gut microbiome of said patient is indicative for a response to said cancer therapy, when compared to a non-responsive patient.

2. The method according to claim 1, wherein said therapy is selected from at least one of a cytotoxic, targeted, and immunotherapy of said patient.

3. The method according to claim 1 or 2, wherein said cancer is selected from breast, colon, lung, ovarian, pancreatic, prostate, and rectal cancer and leukemia.

4. The method according to any one of claims 1 to 3, wherein said detecting the alpha diversity of the gut microbiome comprises at least one of microbiome antigenic profiling, shotgun metagenomic sequencing, PCR, rtPCR, qPCR, multiplex PCR, high-throughput sequencing, metatranscriptomic sequencing, identification of strain-specific markers, such as genes and/or proteins, and 16S rDNA analysis.

5. The method according to any one of claims 1 to 4, wherein said higher alpha diversity in the responding patient is significantly higher, as indicated by a $p < 0.01$, preferably $p < 0.005$ in a Wilcoxon-rank-sum test.

6. The method according to any one of claims 1 to 5, wherein the responding patient exhibits a significantly lower ratio of the phylii Firmicutes/Bacteroidetes (F/B) in said sample.

7. The method according to any one of claims 1 to 6, wherein the responding patient exhibits a significant enrichment of at least one of Bacteroides xylanisolves,

Bacteroides ovatus, Prevotella copri, Alistipes finegoldii, Bacteroides faecis, Bacteroides intestinalis, Biophila wadsworthia, Alistipes indistinctus, Colinsella aerofaciens, Alistipes shahii, Odoribacter splanchnicus, Alistipes putredinis, Bacteriodales bacterium ph8, Eubacterium rectale, Alistipes sp AP11, Parasutterella excrementihominis, Alistipes onderdonkii, Desulfovibrio desulfuricans, Eubacterium ventriosum, Bacteroides fragilis, and Coprococcus cornes in said sample, in particular Bacteroides xylanisolves, and Bacteroides ovatus; and wherein the non-responding patient exhibits a significant enrichment of at least one of Lachnospiraceae bacterium 5 1 57FAA, Lachnospiraceae bacterium 3 1 57FAA CT1, Clostridium spiroforme, Clostridium symbiosum, Anaerotruncuis colihominis, Ruminococcus gnavus, Clostridium hathewayi, Clostridales bacterium 1 7 47FAA, and Erysipelotrichaceae bacterium 21 3 in said sample, in particular Clostridium symbiosum, and Ruminococcus gnavus.

8. The method according to any one of claims 1 to 7, wherein said sample is taken before said treatment as initial sample, or during said treatment.

9. The method according to any one of claims 1 to 8, further comprising a statistical analysis of the KEGG pathways as identified in said sample(s).

10. The method according to any one of claims 1 to 9, further comprising monitoring the progress of said cancer therapy based on said response as detected.

11. A method for identifying a compound suitable for the treatment of cancer, comprising the steps of

a) administering a candidate compound to a mammalian cancer patient, and

b) detecting the alpha diversity of the gut microbiome in a sample obtained from said mammalian cancer patient, and

c) identifying a compound as suitable for the treatment of cancer if a higher alpha diversity of the gut microbiome of said patient is detected in the presence of said compound when compared to the absence of said compound, and

wherein preferably steps a) to c) are repeated, and, optionally, chemically modifying said compound before said repeating.

12. The method according to claim 11, wherein said compound is selected from a cytotoxic, targeted, immunotherapeutic compound, and a composition comprising at least one bacterial species Bacteroides xylanisolves, Bacteroides ovatus, Prevotella copri, Alistipes finegoldii, Bacteroides faecis, Bacteroides intestinalis, Biophila wadsworthia, Alistipes indistinctus, Colinsella aerofaciens, Alistipes shahii, Odoribacter splanchnicus, Alistipes putredinis, Bacteriodales bacterium ph8, Eubacterium rectale, Alistipes sp AP11, Parasutterella excrementihominis, Alistipes onderdonkii, Desulfovibrio desulfuricans, Eubacterium ventriosum, Bacteroides fragilis, and Coprococcus cornes, in particular Bacteroides xylanisolves, and Bacteroides ovatus.

13. A pharmaceutical composition comprising Bacteroides xylanisolves and/or Bacteroides ovatus for use in the treatment of cancer in a mammalian patient.

14. A pharmaceutical composition for use according to claim 13, wherein said treatment comprises a combination treatment with a cytotoxic, targeted, and/or immunotherapy in said patient, in particular kinase inhibitors, such as erlotinib.

15. A method for treating cancer, wherein said treatment is – at least in part – adjusted based on a method according to any one of claims 1 to 12, and/or comprises administering a pharmaceutical composition comprising Bacteroides xylanisolves and/or Bacteroides ovatus to said patient, preferably as a combination treatment with a cytotoxic, targeted, and/or immunotherapy, in particular kinase inhibitors, such as erlotinib.

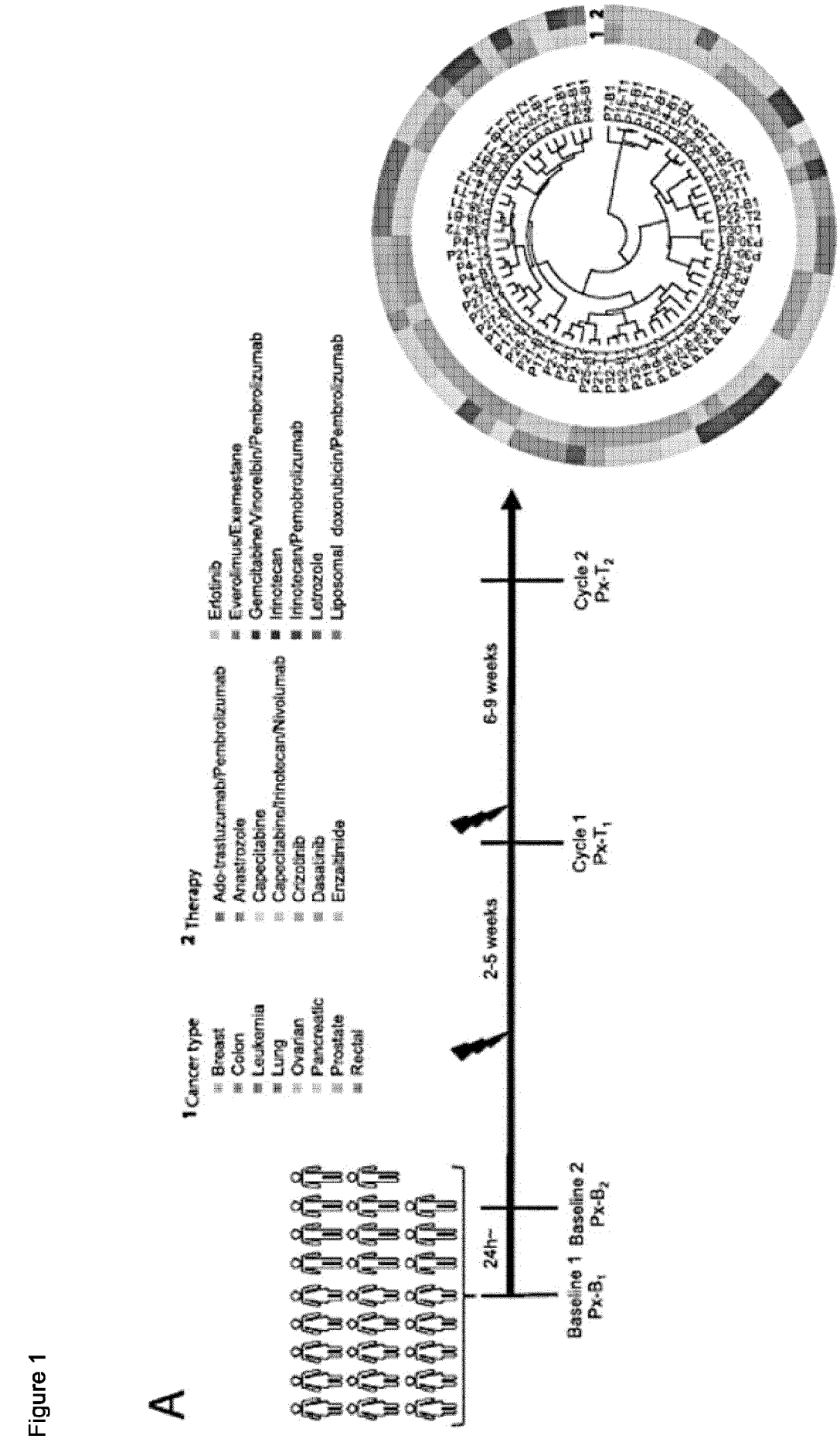
A
1 Cancer type
Breast
Colon
Leukemia
Lung
Ovarian
Pancreatic
Prostate
Rectal
2 Therapy
Ado-trastuzumab/Pembrolizumab
Anastrozole
Capecitabine
Capecitabine/Irinotecan/Nivolumab
Crizotinib
Dasatinib
Enzalimide
Erlotinib
Everolimus/Exemestane
Gemcitabine/Vinorelbin/Pembrolizumab
Irinotecan
Irinotecan/Pemobrolizumab
Letrozole
Liposomal doxorubicin/Pembrolizumab
24h–
2-5 weeks
6-9 weeks
Baseline 1 Px-B1
Baseline 2 Px-B2
Cycle 1 Px-T1
Cycle 2 Px-T2
1
2

Figure 1

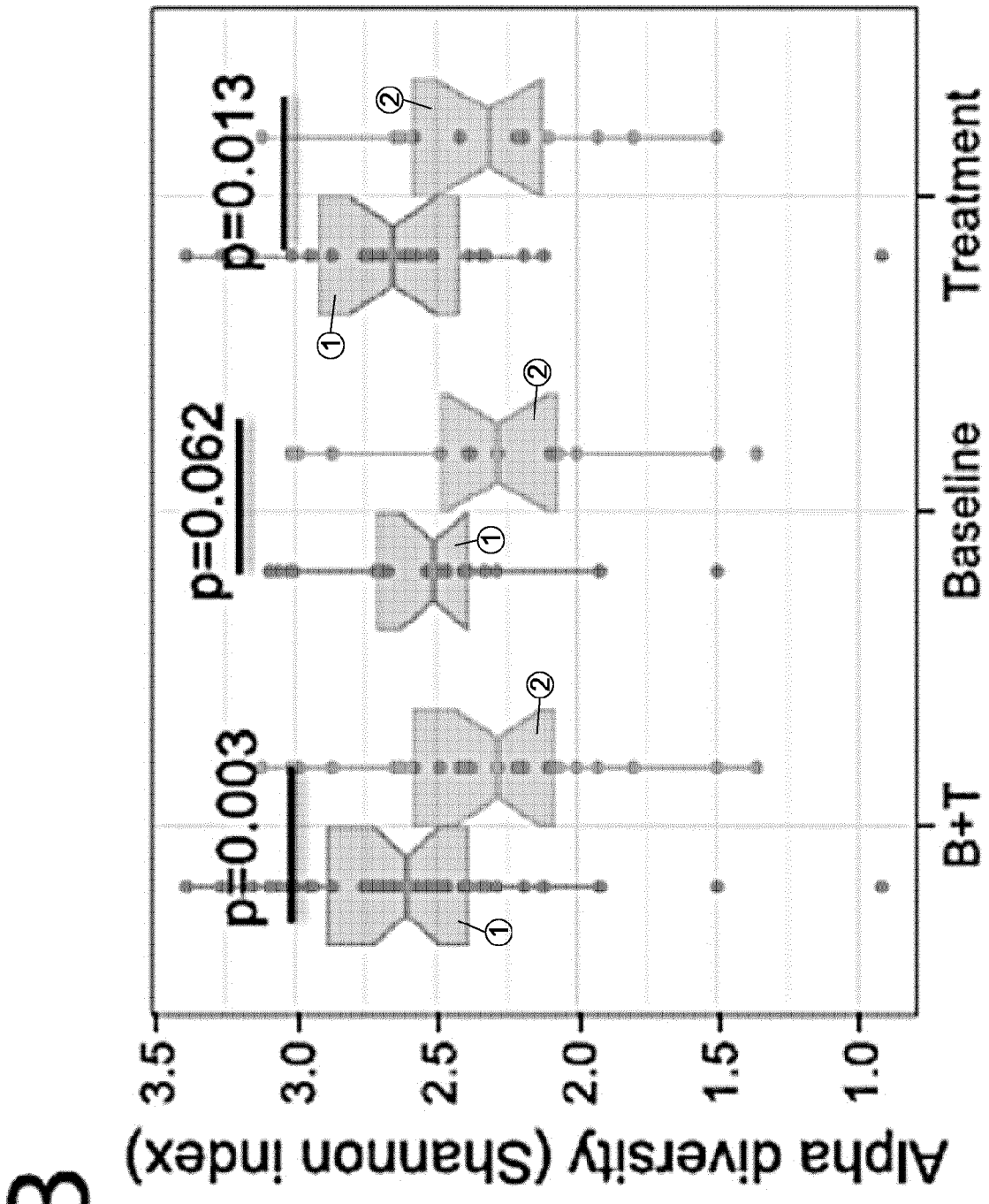

Figure 1(continued)

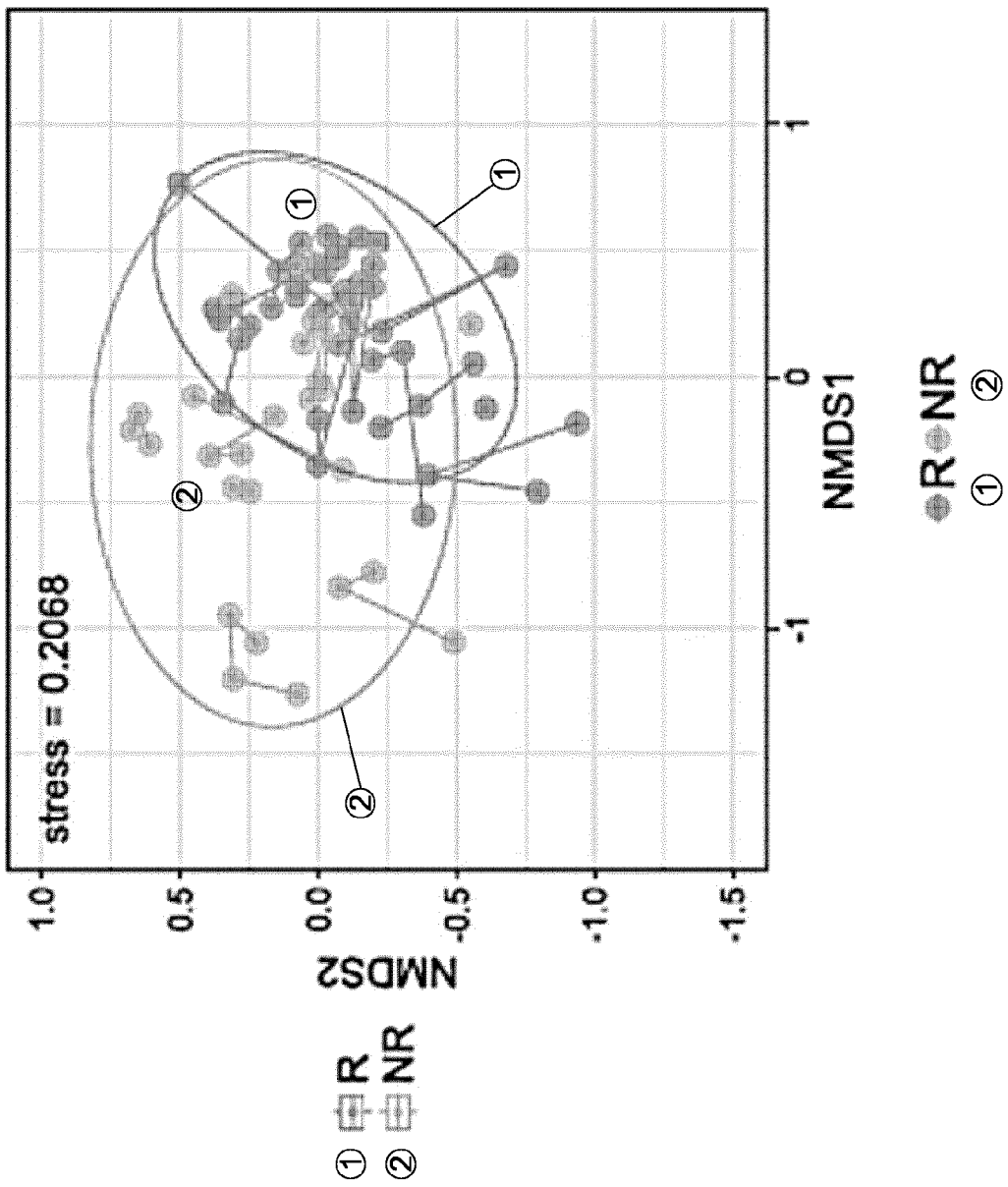

Figure 1(continued)

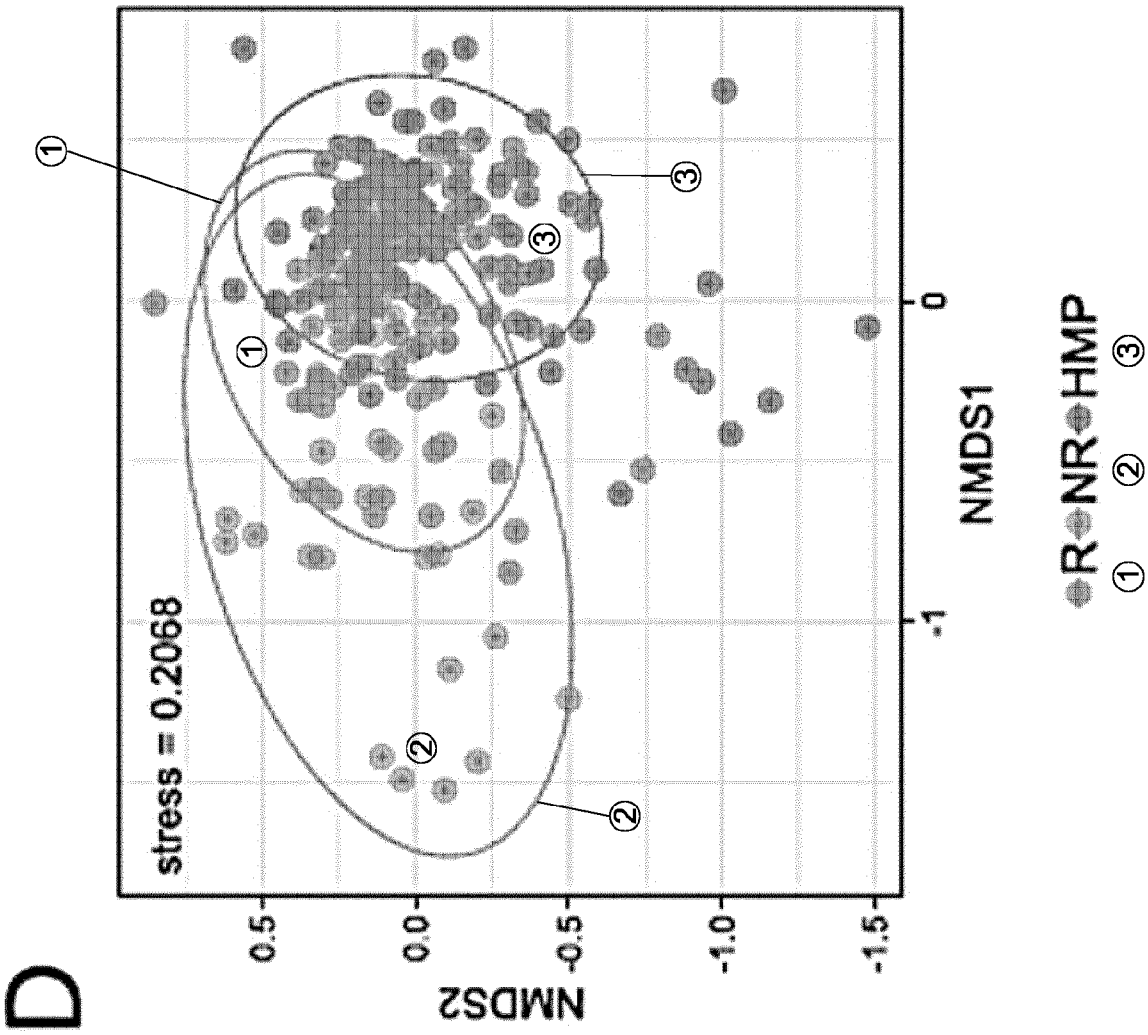

Figure 1(continued)

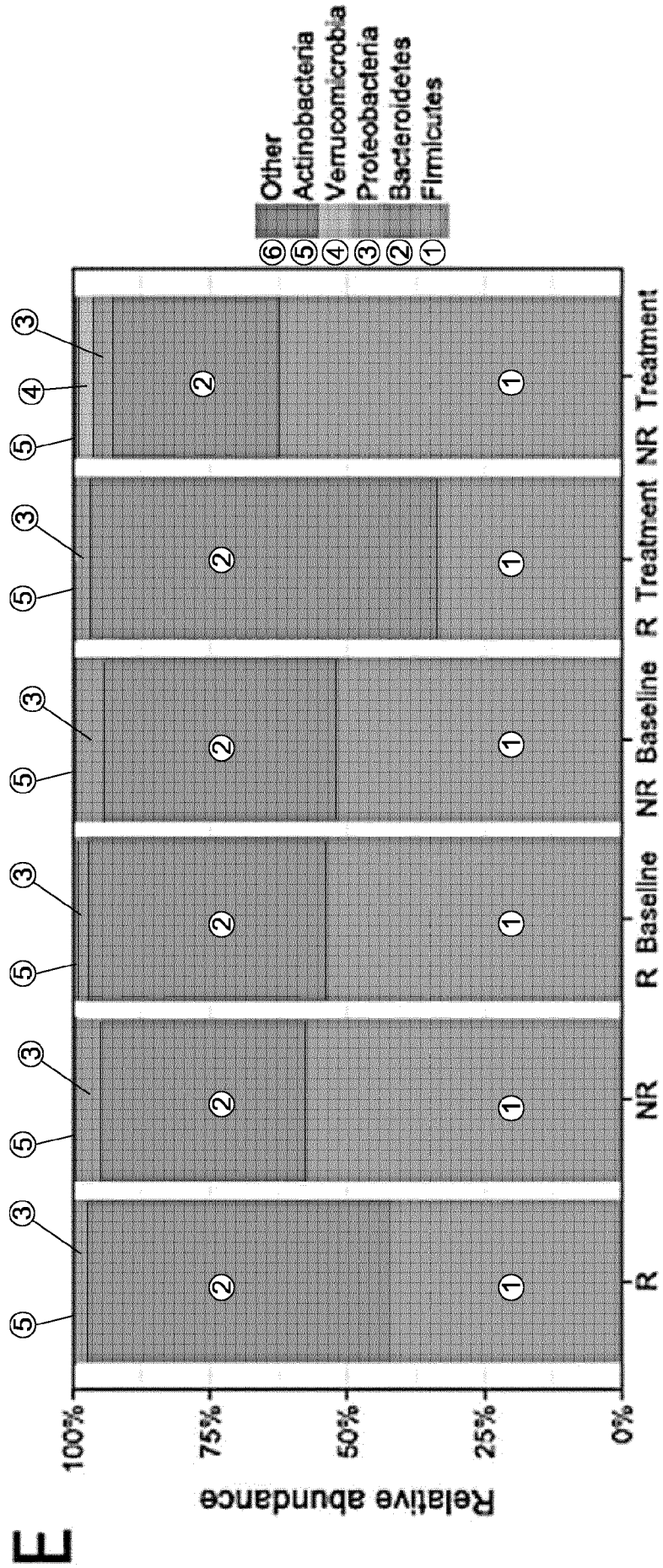

Figure 1(continued)

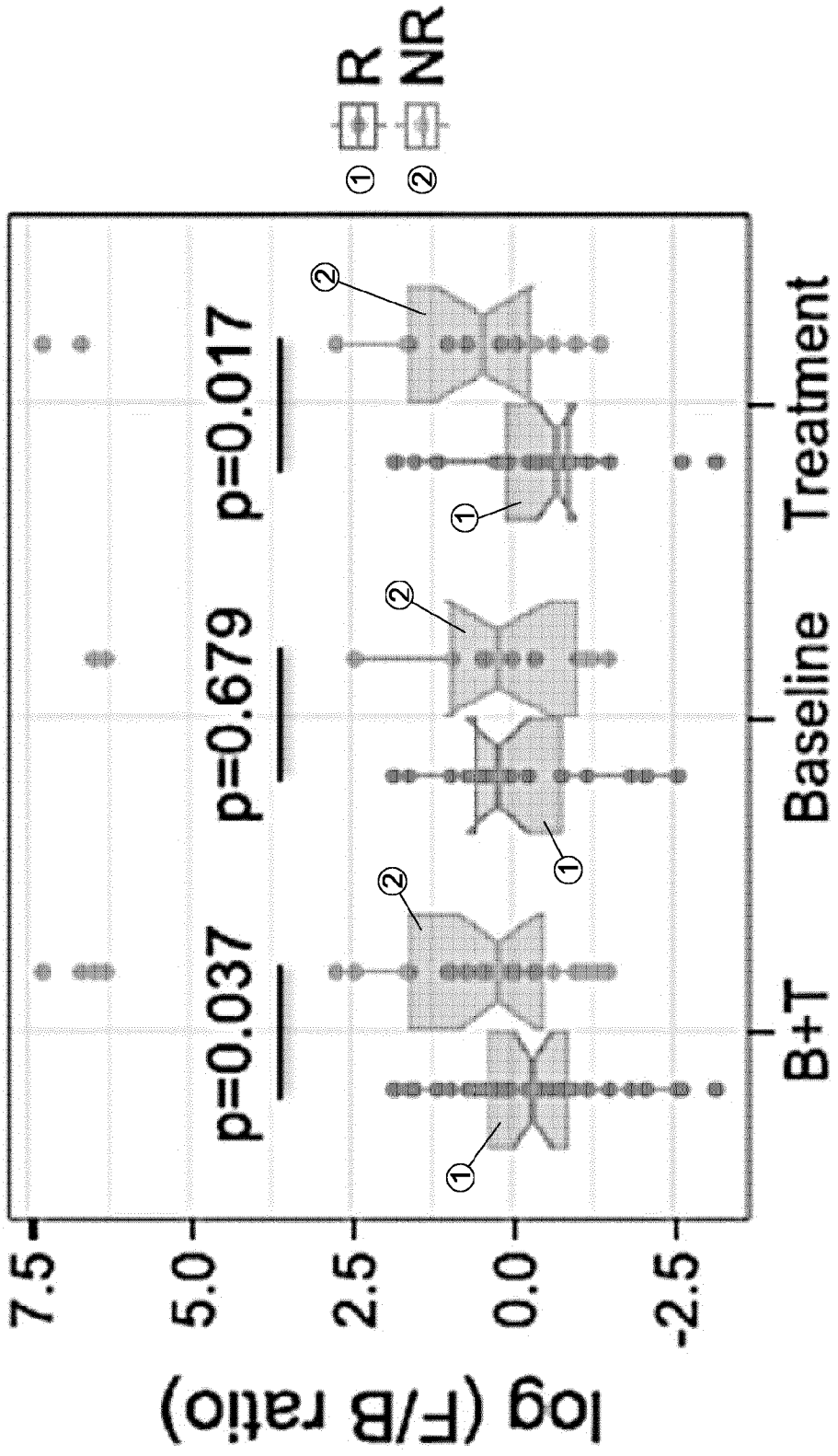

Figure 1(continued)

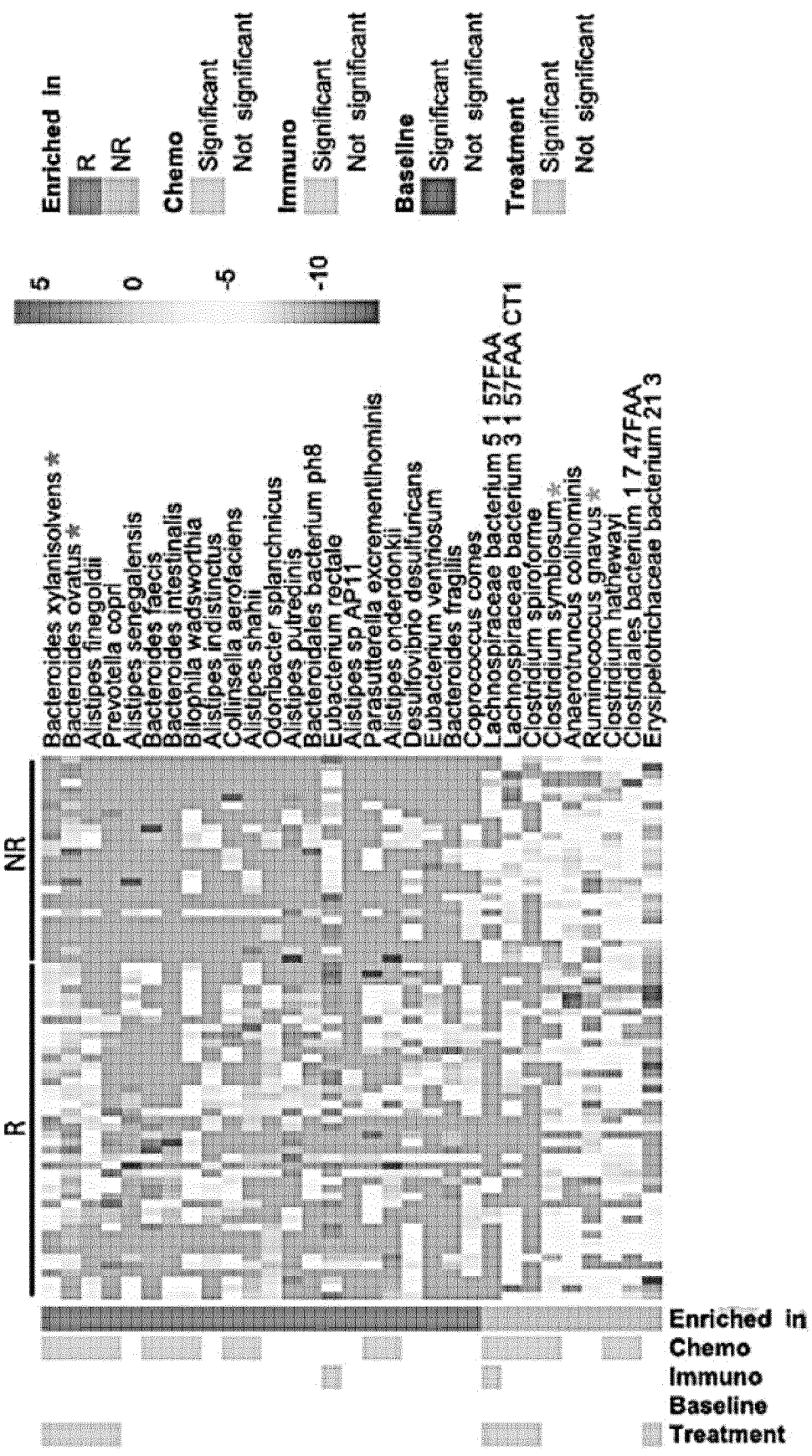

Figure 1(continued)

Figure 2

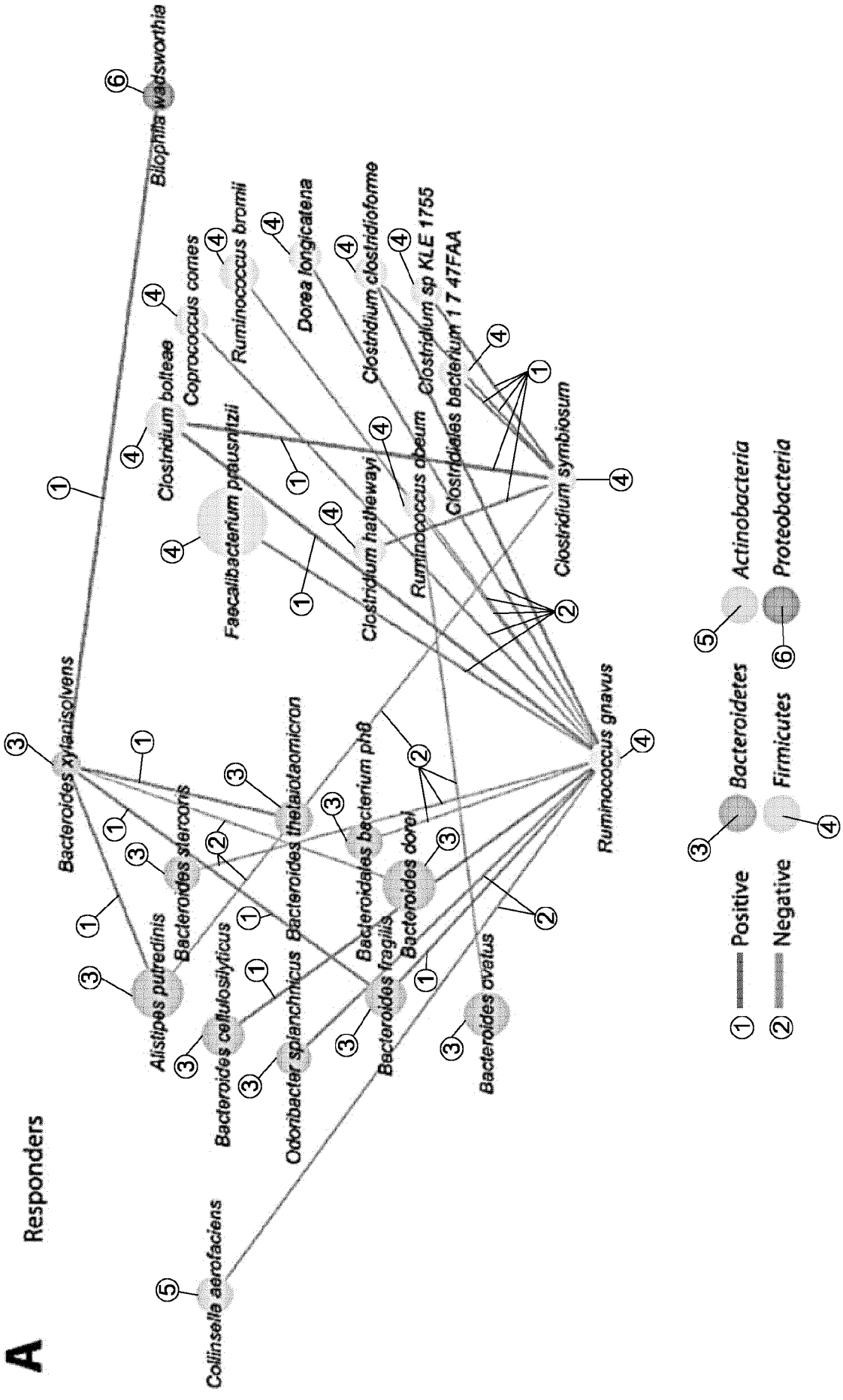
A
Responders
Bilophila wadsworthia
Clostridium bolteae
Coprococcus comes
Ruminococcus bromii
Dorea longicatena
Clostridium clostridioforme
Clostridium sp KLE 1755
Clostridiales bacterium 1 7 47FAA
Faecalibacterium prausnitzii
Clostridium hathewayi
Ruminococcus obeum
Clostridium symbiosum
Bacteroides xylanisolvens
Alistipes putredinis
Bacteroides stercoris
Bacteroides cellulosilyticus
Odoribacter splanchnicus
Bacteroides thetaiotaomicron
Bacteroides fragilis
Bacteroides bacterium ph8
Bacteroides dorei
Bacteroides ovatus
Ruminococcus gnavus
Collinsella aerofaciens
Actinobacteria
Proteobacteria
Bacteroidetes
Firmicutes
Positive
Negative

Figure 2 (continued)

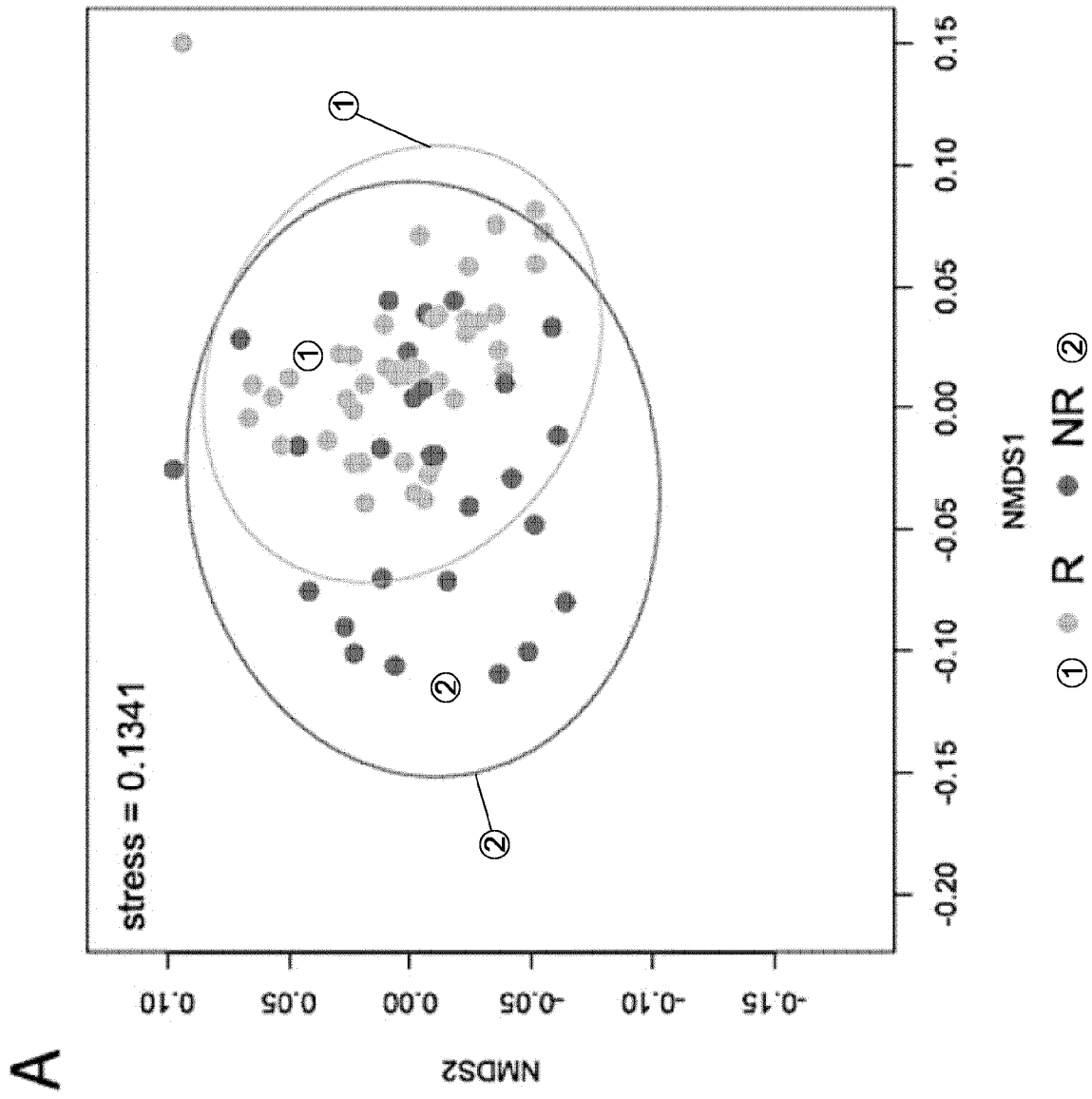
A
NMDS2
0.10
0.05
0.00
-0.05
-0.10
-0.15
NMDS1
0.15
0.10
0.05
0.00
-0.05
-0.10
-0.15
-0.20
stress = 0.1341
① R ② NR
①
②

Figure 3

Figure 3 (continued)

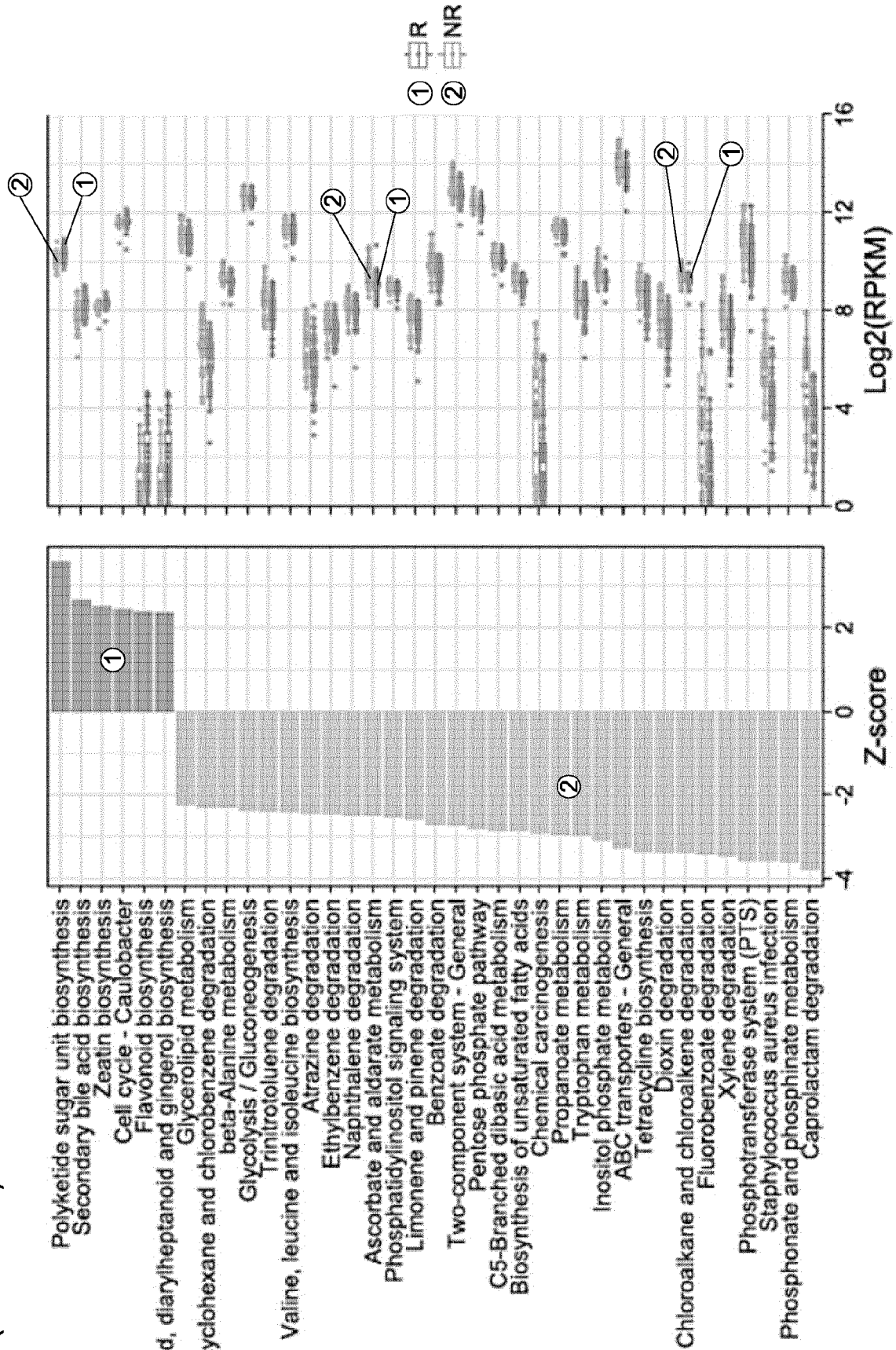

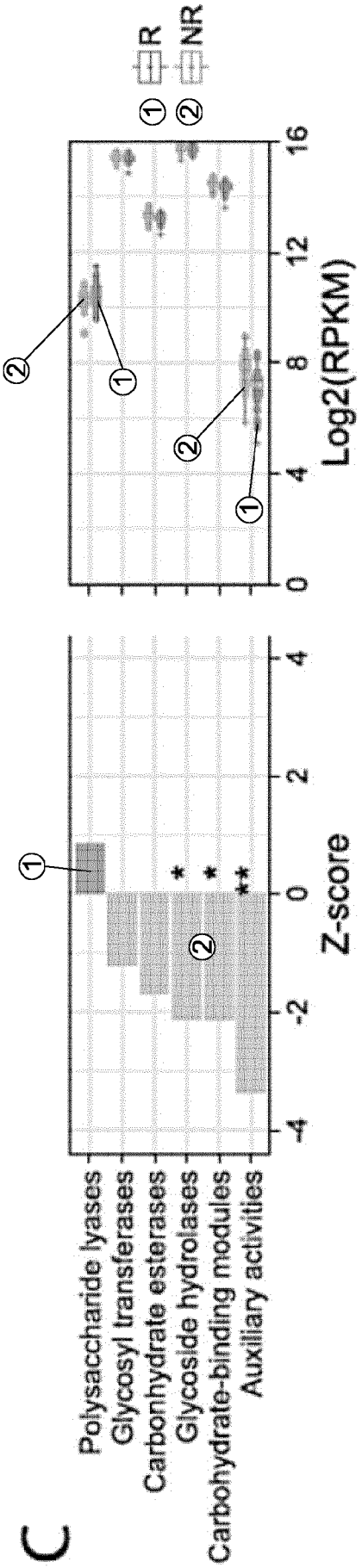

Figure 3 (continued)

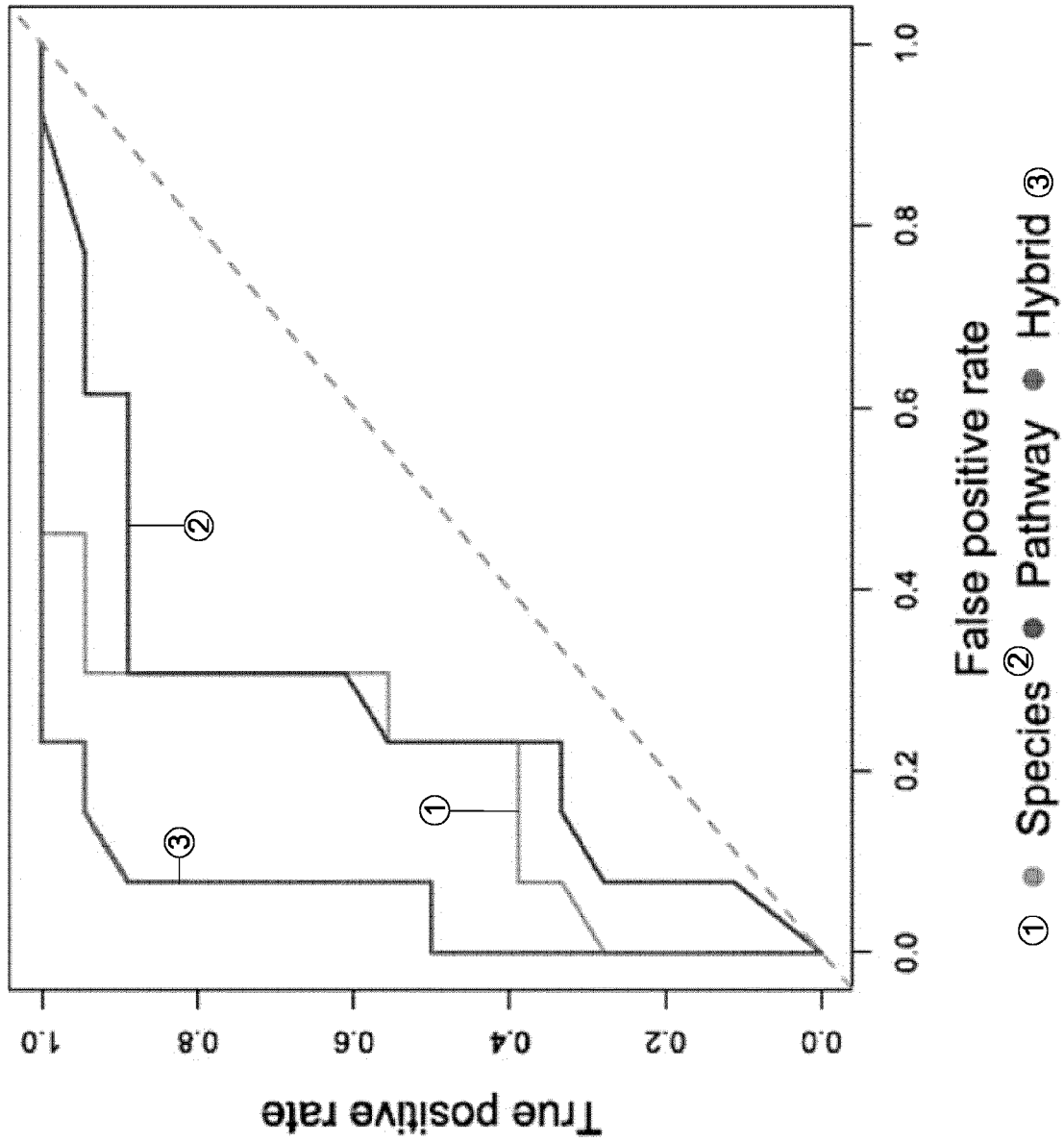

Figure 3 (continued) D

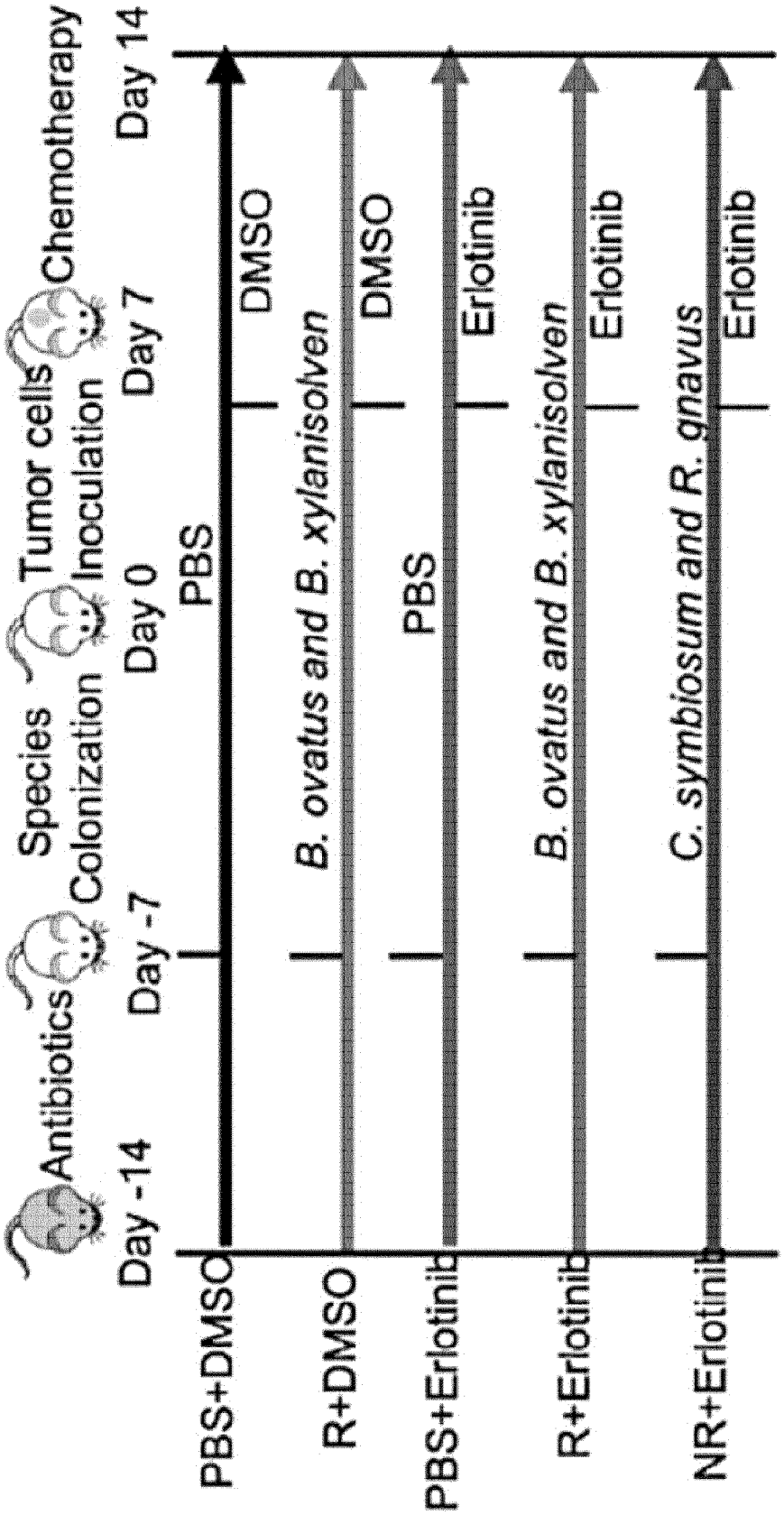
A
Antibiotics
Species Colonization
Tumor cells Inoculation
Chemotherapy
Day -14
Day -7
Day 0
Day 7
Day 14
PBS
DMSO
B. ovatus and B. xylanisolven
PBS
DMSO
Erlotinib
B. ovatus and B. xylanisolven
Erlotinib
C. symbiosum and R. gnavus
Erlotinib
PBS+DMSO
R+DMSO
PBS+Erlotinib
R+Erlotinib
NR+Erlotinib

Figure 4

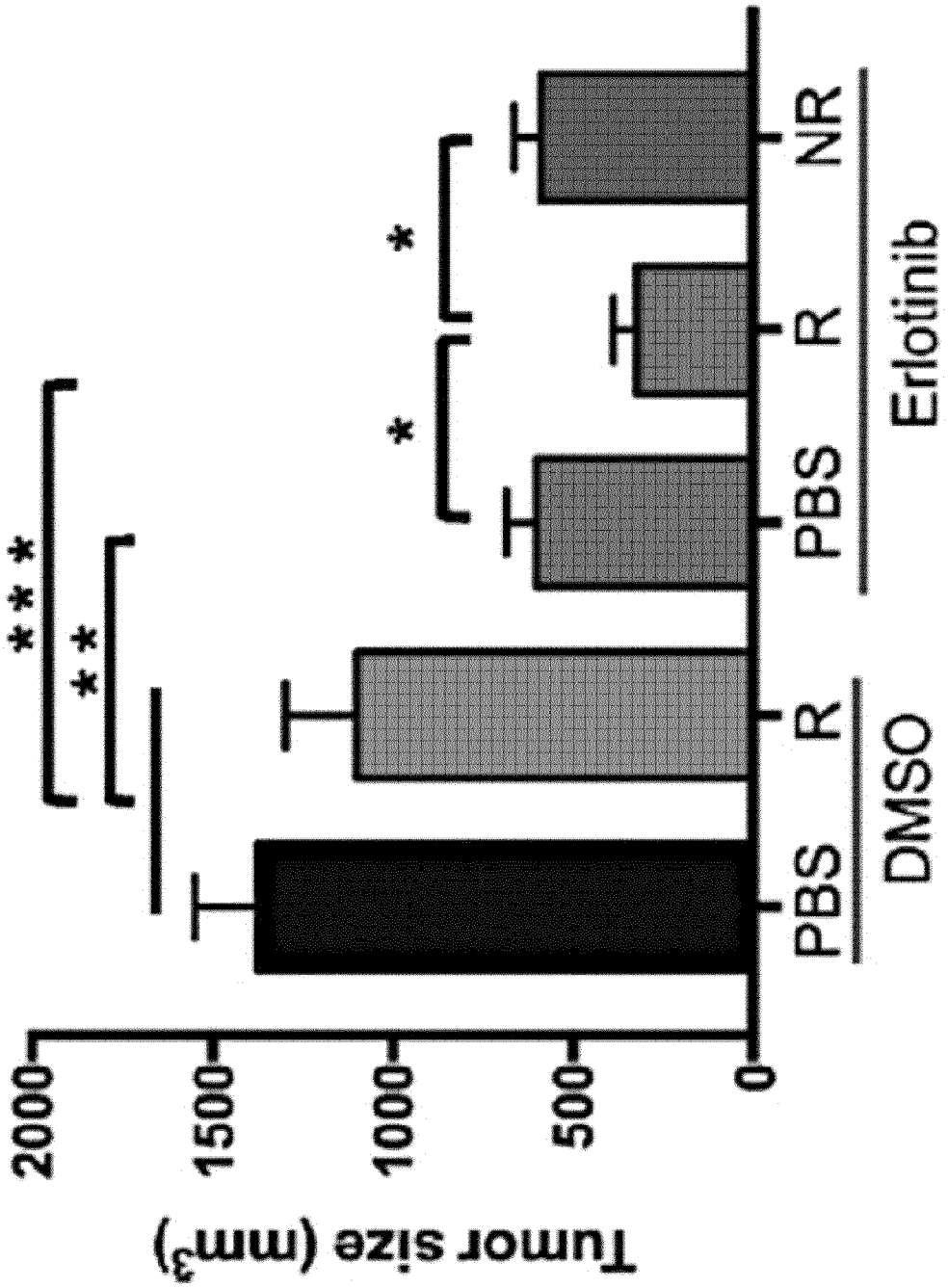

Figure 4 (continued)

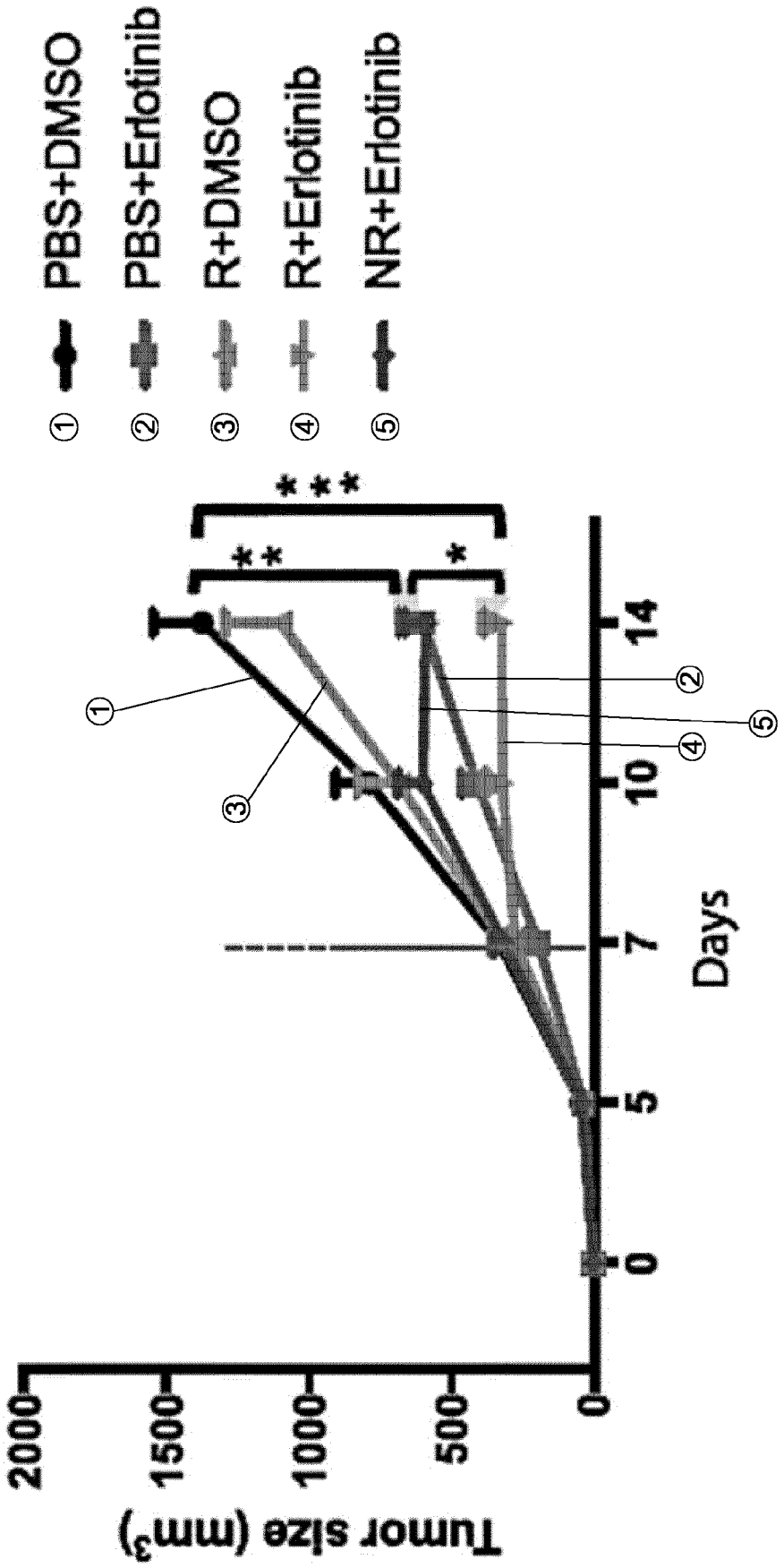

Figure 4 (continued)

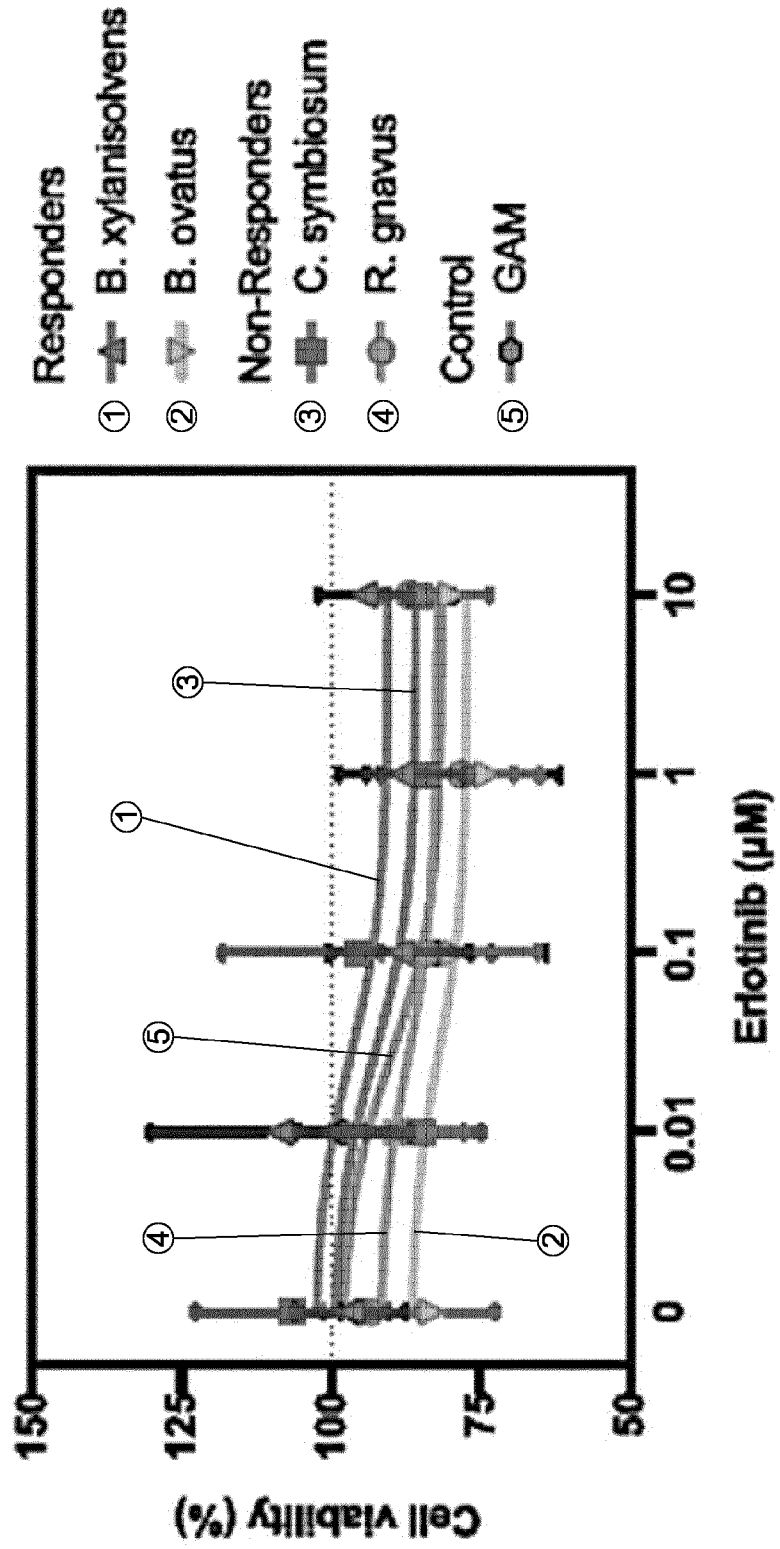

Figure 4 (continued)

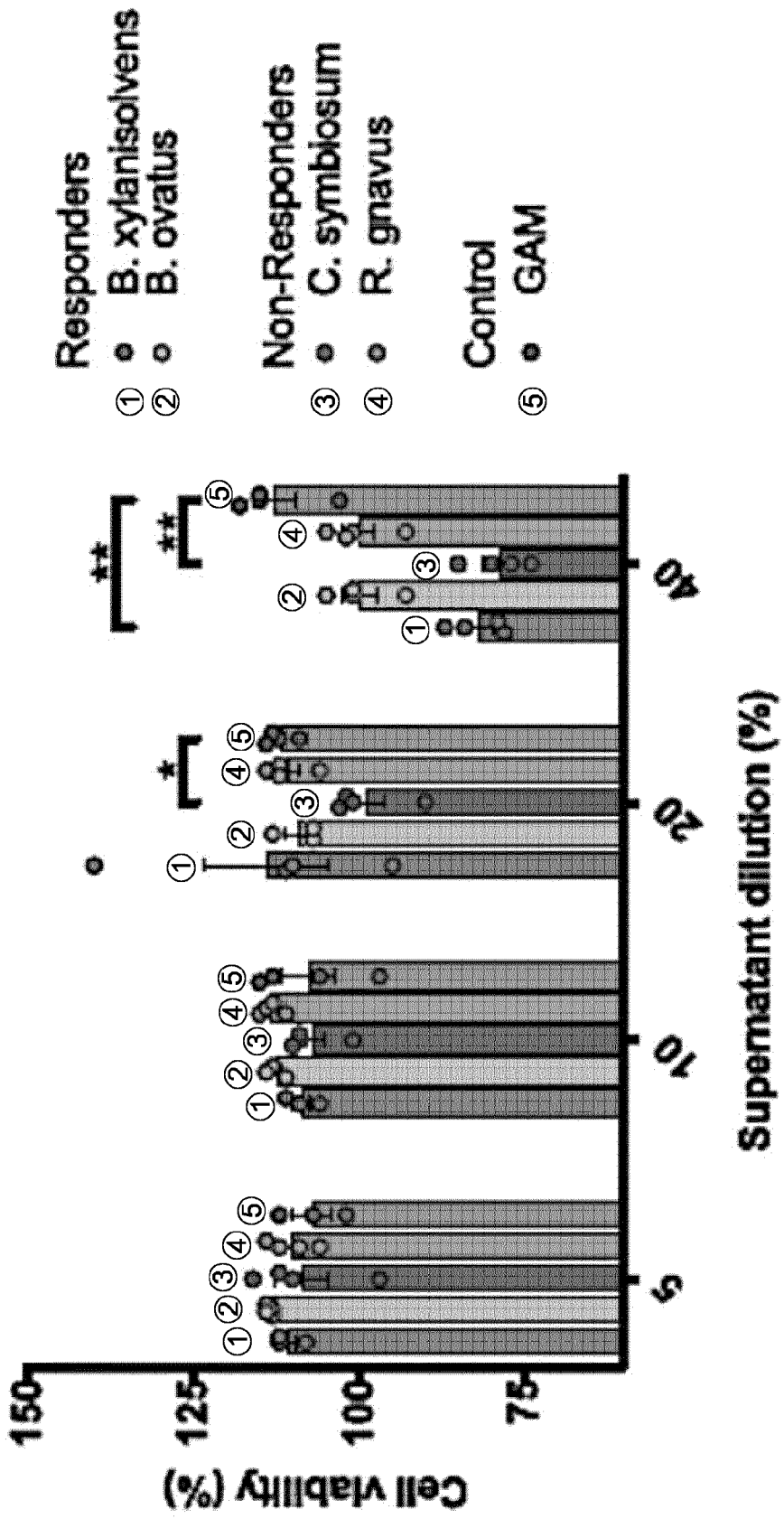

Figure 4 (continued)

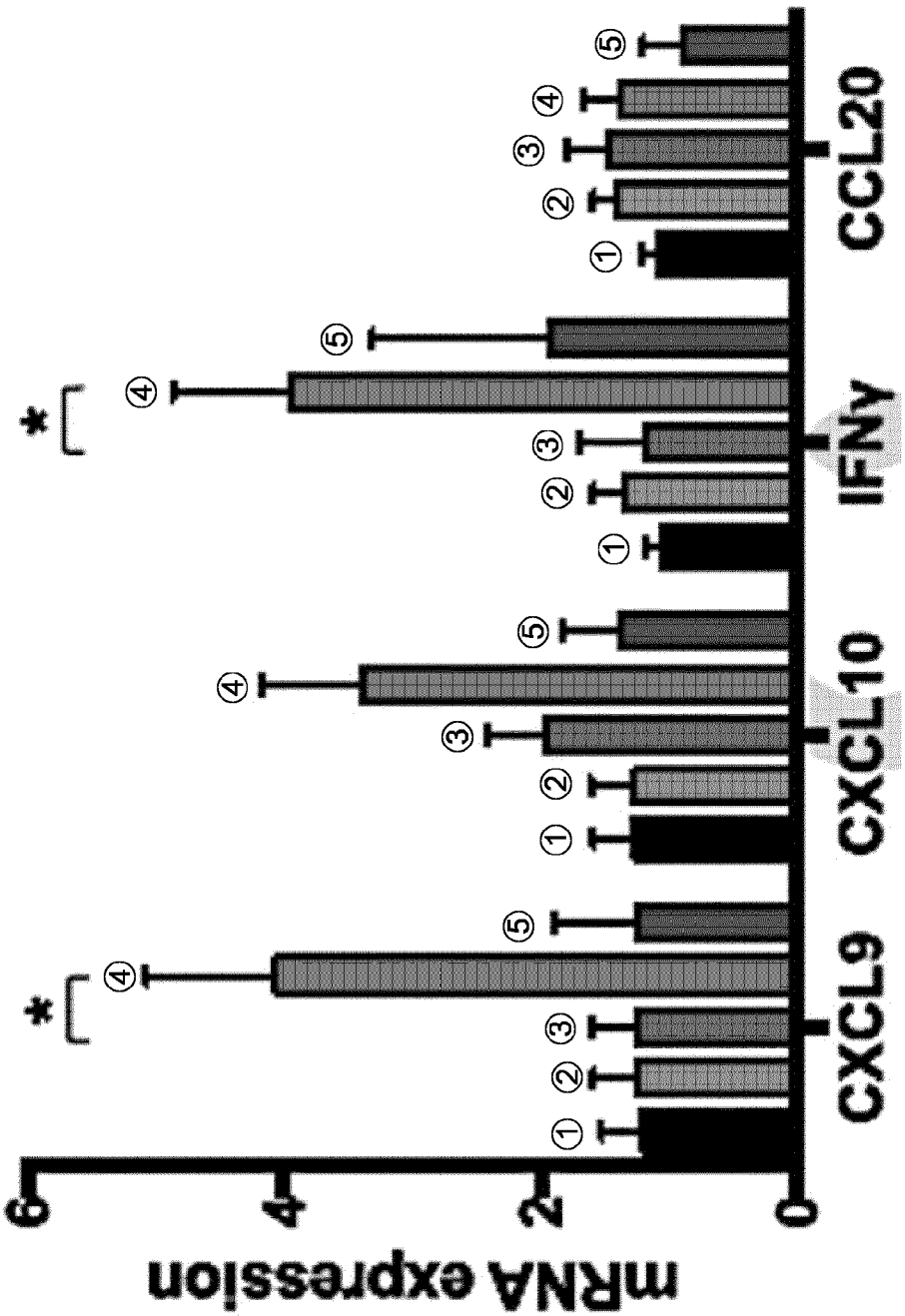

Figure 4 (continued)

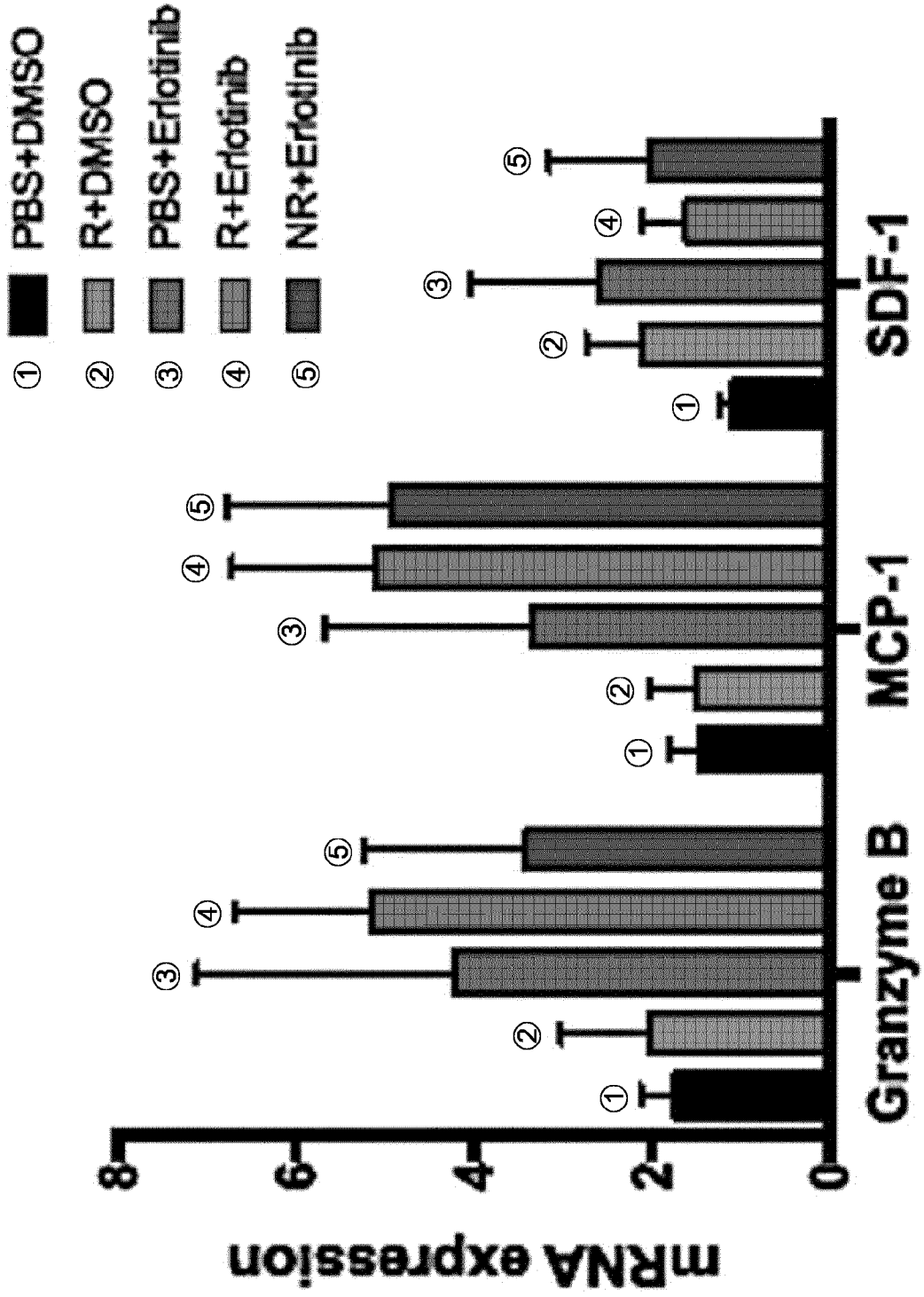

Figure 4 (continued) G

INTERNATIONAL SEARCH REPORT

International application No
PCT/EP2021/055556

A. CLASSIFICATION OF SUBJECT MATTER
INV. C12Q1/6886 C12Q1/689
ADD.

According to International Patent Classification (IPC) or to both national classification and IPC

B. FIELDS SEARCHED

Minimum documentation searched (classification system followed by classification symbols)
C12Q

Documentation searched other than minimum documentation to the extent that such documents are included in the fields searched

Electronic data base consulted during the international search (name of data base and, where practicable, search terms used)
EPO-Internal, BIOSIS, EMBASE, WPI Data

C. DOCUMENTS CONSIDERED TO BE RELEVANT

Category*	Citation of document, with indication, where appropriate, of the relevant passages	Relevant to claim No.
X	YOSHITARO HESHIKI ET AL: "Predictable modulation of cancer treatment outcomes by the gut microbiota", MICROBIOME, BIOMED CENTRAL LTD, LONDON, UK, vol. 8, no. 1, 5 March 2020 (2020-03-05), pages 1-14, XP021274811, DOI: 10.1186/S40168-020-00811-2 the whole document	1-15
X	WO 2018/064165 A2 (UNIV TEXAS [US]) 5 April 2018 (2018-04-05) claims 129, 140, 115, 121	1,2,4,7, 15
X	WO 2018/094190 A2 (SANFORD BURNHAM PREBYS MEDICAL DISCOVERY INST [US] ET AL.) 24 May 2018 (2018-05-24) claims 2, 11, 12	13-15

-/--

[X] Further documents are listed in the continuation of Box C.

[X] See patent family annex.

* Special categories of cited documents :

"A" document defining the general state of the art which is not considered to be of particular relevance

"E" earlier application or patent but published on or after the international filing date

"L" document which may throw doubts on priority claim(s) or which is cited to establish the publication date of another citation or other special reason (as specified)

"O" document referring to an oral disclosure, use, exhibition or other means

"P" document published prior to the international filing date but later than the priority date claimed

"T" later document published after the international filing date or priority date and not in conflict with the application but cited to understand the principle or theory underlying the invention

"X" document of particular relevance; the claimed invention cannot be considered novel or cannot be considered to involve an inventive step when the document is taken alone

"Y" document of particular relevance; the claimed invention cannot be considered to involve an inventive step when the document is combined with one or more other such documents, such combination being obvious to a person skilled in the art

"&" document member of the same patent family

Date of the actual completion of the international search	Date of mailing of the international search report
3 June 2021	09/06/2021

Name and mailing address of the ISA/	Authorized officer
European Patent Office, P.B. 5818 Patentlaan 2 NL - 2280 HV Rijswijk Tel. (+31-70) 340-2040, Fax: (+31-70) 340-3016	Santagati, Fabio

2

Form PCT/ISA/210 (second sheet) (April 2005)

C(Continuation). DOCUMENTS CONSIDERED TO BE RELEVANT

Category*	Citation of document, with indication, where appropriate, of the relevant passages	Relevant to claim No.
X	WO 2019/149859 A1 (UNIV BASEL [CH]) 8 August 2019 (2019-08-08) claims 1,2,8, 11,14	13-15
X	V. GOPALAKRISHNAN ET AL: "Gut microbiome modulates response to anti-PD-1 immunotherapy in melanoma patients", SCIENCE, vol. 359, no. 6371, 5 January 2018 (2018-01-05), pages 97-103, XP055554925, US ISSN: 0036-8075, DOI: 10.1126/science.aan4236 the whole document	1,2,4
X	JIN YUEPING ET AL: "The Diversity of Gut Microbiome is Associated With Favorable Responses to Anti-Programmed Death 1 Immunotherapy in Chinese Patients With NSCLC", JOURNAL OF THORACIC ONCOLOGY, vol. 14, no. 8, 1 August 2019 (2019-08-01) , pages 1378-1389, XP055809261, US ISSN: 1556-0864, DOI: 10.1016/j.jtho.2019.04.007 the whole document	1-4

INTERNATIONAL SEARCH REPORT

International application No.
PCT/EP2021/055556

Box No. I Nucleotide and/or amino acid sequence(s) (Continuation of item 1.c of the first sheet)

1. With regard to any nucleotide and/or amino acid sequence disclosed in the international application, the international search was carried out on the basis of a sequence listing:

   a. [X] forming part of the international application as filed:

      [X] in the form of an Annex C/ST.25 text file.

      [ ] on paper or in the form of an image file.

   b. [ ] furnished together with the international application under PCT Rule 13*ter*.1(a) for the purposes of international search only in the form of an Annex C/ST.25 text file.

   c. [ ] furnished subsequent to the international filing date for the purposes of international search only:

      [ ] in the form of an Annex C/ST.25 text file (Rule 13*ter*.1(a)).

      [ ] on paper or in the form of an image file (Rule 13*ter*.1(b) and Administrative Instructions, Section 713).

2. [ ] In addition, in the case that more than one version or copy of a sequence listing has been filed or furnished, the required statements that the information in the subsequent or additional copies is identical to that forming part of the application as filed or does not go beyond the application as filed, as appropriate, were furnished.

3. Additional comments:

INTERNATIONAL SEARCH REPORT

Information on patent family members

International application No
PCT/EP2021/055556

Patent document cited in search report	Publication date	Patent family member(s)	Publication date
WO 2018064165 A2	05-04-2018	AU 2017335732 A1	04-04-2019
		BR 112019006041 A2	03-09-2019
		CA 3038076 A1	05-04-2018
		CN 110267651 A	20-09-2019
		EP 3518946 A2	07-08-2019
		JP 2020500151 A	09-01-2020
		KR 20190061042 A	04-06-2019
		RU 2019108925 A	29-10-2020
		US 2020129569 A1	30-04-2020
		WO 2018064165 A2	05-04-2018
WO 2018094190 A2	24-05-2018	EP 3541400 A2	25-09-2019
		US 2019365829 A1	05-12-2019
		WO 2018094190 A2	24-05-2018
WO 2019149859 A1	08-08-2019	NONE	